AN EXPERIMENTAL STUDY AIMING TO ENHANCE THE PERFORMANCE OF OSR OF A FUEL PROCESSOR

by

Cihat Öztepe

B.S., Chemical Engineering, Boğaziçi University, 2015

Submitted to the Institute for Graduate Studies in
Science and Engineering in partial fulfillment of
the requirements for the degree of
Master of Science

Graduate Program in Chemical Engineering

Boğaziçi University

2017

not to the ignorance

ACKNOWLEDGEMENTS

First of all, I would like to express my sincere gratitude to my thesis supervisor Prof. Ahmet Erhan Aksoylu for his motivation, guidance and support. It was a great experience to work with him beacuse I have learned a lot from his knowledge, expertise and wisdom in catalysis, reaction engineering.

I am very grateful to Dr. Burcu Selen Çağlayan for her perpetual help, guidance and suggestions throughout my work.

I wish to express my sincere appreciations for the members of thesis committee, Prof. Hüsnü Atakül and Assoc. Prof. Hasan Bedir, for accepting to be a member of the thesis committee, devoting their valuable time to read and comment on my thesis.

I would like to thank Dr. Melek Selcen Başar for her instructions and assistance from the beginning of my experimental and computational work. Also very special thanks for Belkız Merve Eropak and Ali Uzun for their great help whenever I needed it.

I also wish to express my gratitude to Aybüke Leba, Dr. Aysun İpek Paksoy, the CATREL team and also former members of KB 403.

I also thank my friends Sercan Altundemir, Ayşe Eren, Ahmet Hallaçeli, Ece Çiğdem Mutlu, Gözde Öztürk, Ayça Soylu for their frienships through my M.Sc. years.

Cordial thanks for Bilgi Dedeoğlu, Yakup Bal, Murat Düzgünoğlu, Melike Gürbüz and Başak Ünen for their technical assistance and help.

Finally, I wish to thank my family; my father, my grandmother, and my grandfather.

Financial support for this study was provided by TÜBİTAK through project 215M312. The financial support provided for lab infrastructure by Republic of Turkey Ministry of Development through project 2016K121160 is greatly acknowledged.

ABSTRACT

AN EXPERIMENTAL STUDY AIMING TO ENHANCE THE PERFORMANCE OF OSR OF A FUEL PROCESSOR

The aim of this study is to determine the optimum operating parameters of the methane OSR unit of the Fuel Processor Prototype-FPP yielding high methane conversion activity with suppressed H_2/CO product selectivity through a Box-Behnken experimental design using temperature, S/C and O/C ratios of the feed, and the catalyst weight (or residence time, W/F) as the experimental parameters. The ranges of 350-450 °C, 3-5, 0.74-1.33, and 1.50-2.00 mg.min/ml were used as the experimental design parameter ranges for temperature, S/C feed ratio, O/C feed ratio and W/F, respectively. Additionally, a thermodynamic analysis was also performed for the same operation conditions in order to form a comparison basis for evaluating the performance test results, and for better understanding of the nature of OSR as well. Experimental CH_4 conversion was increased by a rise in each of the parameters of temperature, S/C and O/C feed ratios; and this trend was confirmed via the thermodynamic analysis for the conditions used in the experiments. On the other hand, the observed effect of W/F on experimental CH_4 conversion was nonconventional, i.e. an increase in W/F mostly resulted in a decrease in CH_4 conversion. This was confirmed further by comparative analysis with the thermodynamic simulation results yielding lower CH_4 conversion levels compared to those obtained in the experiments for W/F ratios of 1.50-2.00 mg.min/ml. In addition to CH_4 conversion, product distribution of OSR varied with the changes in the reaction conditions. Consequently, as the trends in H_2 production and H_2/CO product ratio obtained as a function of W/F were -in general- opposite, the results reveal the existence of a Pareto optimal for W/F value, and strongly suggested the necessity of scrutinizing the relation between space time/space velocity (W/F) and reactor performance to find the practical operating conditions for the OSR reactor.

ÖZET

BİR YAKIT İŞLEMCİSİNİN OBR PERFORMASINI ARTIRMAYI AMAÇLAYAN DENEYSEL BİR ÇALIŞMA

Bu çalışmanın amacı, deneysel parametreler olarak sıcaklık, buhar/karbon besleme oranı (S/C), oksijen/karbon besleme oranı (O/C) ve katalizör ağırlığını (veya kalma süresi, W/F) kullanan bir Box-Behnken deney dizaynı vasıtası ile, yüksek metan çevrim aktivitesini bastırılmış H_2/CO ürün seçiciliğiyle sağlayan bir yakıt işlemcisi prototipinin-FPP metan oksidatif buhar reformlama (OBR) unitesinin optimum çalışma parametrelerini belirlemektir. 350-450 °C, 3-5, 0.74-1.33, and 1.50-2.00 mg.dk/ml aralıkları sırasıyla, sıcaklık, buhar/karbon besleme oranı, oksijen/karbon besleme oranı ve kalma süresi parametrelerinin deneysel aralıkları olarak kullanılmıştır. Ek olarak, performans test sonuçlarını değerlendirmek için bir kıyaslama temeli oluşturmak ve OBR'nin mahiyetini daha iyi anlamak adına, aynı koşullarda bir termodinamik analiz yapıldı. Deneysel CH_4 çevrimi, sıcaklık, buhar/karbon ve oksijen/karbon besleme oranları parametrelerinin ayrı ayrı her birinin artırılmasıyla arttı; ve bu eğilim deneylerde kullanılan koşullar için yapılan termodinamik analizle teyit edildi. Öte yandan, kamla süresinin CH_4 çevrimindeki gözlenen etkisi alışılagelmemiş şekildeydi, diğer bir deyişle kalma süresindeki bir artış CH_4 çevriminde bir düşüşe sebep oldu. Bu durum, deneylerde 1.50-2.00 mg.dk/ml kalma süresi için elde edilenlere kıyasla daha düşük CH_4 çevrim seviyeleri veren termodinamik simulasyonlu kıyaslama analiziyle ayrıca teyit edildi. Metan çevrimine ek olarak, OBR'nin ürün dağılımı da reaksiyon koşularına göre farklılık gösterdi. Sonuç olarak, kalma süresine bağlı olarak elde edilen H_2 üretimi ve H_2/CO ürün oranı trendleri -genelde- aksi yönde oldukları için; sonuçlar, hem kalma süresi için bir Pareto optimali olduğunu ortaya çıkardı hem de OBR reaktörü için uygulanabilir çalışma koşullarını bulmak adına, kalma süresi ile reaktör performası arasındaki ilişkinin ince elenip sık dokunması gerekliliğini güçlü bir şekilde ortaya koydu.

TABLE OF CONTENTS

LIST OF FIGURES

LIST OF TABLES

LIST OF SYMBOLS

F	Molar flow rate
O/C	Oxygen-to-carbon ratio
O/M	Oxygen-to-methane ratio
P	Pressure
Q	Heat
S/C	Steam-to-carbon ratio
S/M	Steam-to-methane ratio
T	Temperature
W	Work
W/F	Residence time
ΔH	Enthalpy of reaction
$\Delta H^{\circ}_{25°C}$	Standard enthalpy of reaction

LIST OF ACRONYMS/ABBREVIATIONS

AFC	Alkaline Fuel Cell
ATR	Autothermal Reforming
CATREL	Catalysis and Reaction Engineering Laboratory
DI	Deionized
DMFC	Direct Methanol Fuel Cell
EDX	Energy Dispersive using X-ray
FC	Fuel Cell
FP	Fuel Processor
FPP	Fuel Processor Prototype
FT	Flow Through
GHSV	Gas Hourly Space Velocity
HPLC	High Performance Liquid Chromatography
HTS	High Temperature Shift
ID	Inner Diameter
LPG	Liquefied Petroleum Gas
LTS	Low Temperature Shift
MCFC	Molten Carbonate Fuel Cell
MFC	Mass Flow Controller
OD	Outer Diameter
OSR	Oxidative Steam Reforming
PAFC	Phosphoric Acid Fuel Cell
PEM	Proton Exchange Membrane
PEMFC	Proton Exchange Membrane Fuel Cell
POX	Partial Oxidation
PROX	Preferential Oxidation
r-HTS	Reverse High Temperature Shift
SEM	Scanning Electron Microscope
SMET	Selective Methanation
SOFC	Solid Oxide Fuel Cell

SR	Steam Reforming
SS	Stainless Steel
TEM	Transmission Electron Microscope
TOS	Time-on-stream
TOX	Total Oxidation
TPR	Temperature-Programmed Reduction
WGS	Water-Gas Shift
WF	Wall Flow
WSV	Weight hourly Space Velocity
XRD	X Ray Diffraction

1. INTRODUCTION

Today's preponderant global energy sources are fossil fuels, including oil, natural gas, coal; however, their usage in the energy sector is questionable due to their high CO_2 and methane emissions (Heede and Oreskes, 2016). Considering anthropogenic climate change, alternative ways of energy production, as replacements of fossil based sources in satisfying global energy demand, are desired. One of these alternative energy production ways is fuel cell technology which was invented by William Grove in 1839 (Behling, 2013). Fuel cell technology is a promising option to produce energy in satisfying the global demand, especially for small scale stationary operations.

The fuel cells in general are classified according to their feed type, specifications and operating conditions. The best fuel cell option to be used in small scale stationary operations is polymer electrolyte membrane fuel cells (PEMFC) with its high energy intensity and compactness (Behling, 2013). The main problem related with the use of PEMFC is its fuel; PEMFC needs hydrogen having CO concentration lower than 100 ppm for its stable operation.

The use of stored hydrogen in a PEMFC is not feasible due to both safety concerns for pressurized, and high volume requirement for non-pressurized hydrogen storage, especially for distributed energy production via small scale operations. As well-established hydrogen distribution network is not available, on-site production of hydrogen from easy-to-store and/or easy-to-distribute hydrocarbons for small scale stationary applications by the use of a fuel processor (FP) is one of the plausible options. A typical FP involve catalytic hydrogen production (reformer) and enriching/purification (water gas shift, WGS; preferential oxidation, PROX) units in series (Moreno *et al.*, 2015).

The primary element of fuel processor is reforming unit producing hydrogen-rich effluent gas stream from a conventional fuel. The composition of the effluent depends on the type of fuel, properties of the catalyst(s), operation conditions, and application area as well. Main reforming reaction types are steam reforming (SR), partial oxidation (POX) or oxidative steam reforming (OSR); the latter is called autothermal reforming (ATR) when the

reformer unit does not need additional heat during its steady state operation. The hydrogen-rich effluent stream of reforming unit also contains CO for all above mentioned reforming reaction cases. As PEMFC operates at low temperatures, in the range of 80-95 ˚C, and its platinum anode is highly prone to CO poisoning for that temperature range, an FP of a combined FP-PEMFC system must also include a water-gas-shift (WGS) unit for decreasing CO concentration of the reformer effluent while increasing its hydrogen content, and a following preferential oxidation (PROX) unit for reducing CO concentration further, less than 100 ppm, for stable PEMFC operation (Cipiti *et al.*, 2013; Kalmula and Kondapuram, 2015).

There are several studies about FP systems, even combined FP-PEMFC systems, in the literature. For instance, a research group from Republic of Korea, Wang Lai Yoon *et al.*, studied fuel processor units for residential FP-PEMFC systems by using natural gas as the fuel for stationary applications. Their FP had a reformer, two stage WGS units and a PROX unit, and they presented activity and performance results of the systems (Seo *et al.*, 2006a; Seo *et al.*, 2006b; Jung *et al.*, 2014). Moreover, another research group from Italy, Specchia *et al.*, studied fuel processor systems for PEMFC for mobile/vehicle applications, and used iso-octane, diesel, bio-diesel and methanol as the fuels. They examined the use of both ATR and SR in the reformer and the use of PROX and selective methanation of CO as CO-cleaning unit (Sgroi *et al.*, 2005; Cutillo *et al.*, 2006; Icardi *et al.*, 2008; Kolb *et al.*, 2008; Asharf *et al.*, 2014; Ercolino *et al.*, 2015).

Our group has developed several promising catalysts for the OSR, WGS and PROX units of a FP system. Power-law type kinetic expressions over the ones showed the highest performance in the FP reactions have also been attained by our group. Besides, a fuel processor prototype (FPP) had been constructed by a member of our group, and she had studied individual performances of the catalysts as well as their serial OSR-WGS, OSR-PROX and OSR-WGS-PROX performance in the FPP for propane feed (Başar, 2016).

Pt-Ni/δ-Al_2O_3 catalyst (Çağlayan *et al.*, 2005; Gökaliler *et al.*, 2008; Gökaliler *et al.*, 2012) has been designed for OSR reaction, and its formulation has been optimized on the basis of its performance, i.e. activity, selectivity and stability characteristics. A reliable power law type kinetic expression has been obtained for methane OSR over the Pt-Ni

catalyst under realistic conditions (Erdinç *et al.,* 2017). The aim of the current thesis is to determine the optimum operating parameters of the methane OSR unit of the Fuel Processor Prototype-FPP yielding high methane conversion activity with suppressed H_2/CO product selectivity via an experimental study using temperature, S/C and O/C ratios of the feed, and the catalyst weight (or residence time, W/F) as the experimental parameters whose levels were determined by Box-Behnken experimental design. Additionally, a thermodynamic analysis was also conducted for the same operation conditions in order to form a comparison basis for evaluating the performance test results, and for better understanding of the nature of OSR as well.

Chapter 2 comprises a literature survey including a brief information about fuel cells, an explanation of fuel processor reactions and a detailed information of fuel processor systems and separate oxidative steam reforming/autothermal reforming units with their parametric and thermodynamic analyses in the literature. Experimental systems, catalyst preparation and pretreatment procedures, and reaction tests for this study are presented in Chapter 3. Chapter 4 contains the results of performance analyses of the system with thermodynamic comparisons and discussions of these results. Lastly, the conclusions deduced from the findings in this study and recommendations for the future studies related to this topic are given in Chapter 5.

2. LITERATURE SURVEY

2.1. Fuel Cells

Fuel cells (FCs), which are one of the oldest electrical energy producing methods, were invented in the middle of 19th century. One of the main motivations of developing fuel cell technology is to prevent harmful environmental effects of fossil fuels burnt to obtain energy by replacing fossil fuel consumption with electrical energy conversion via fuel cells. Fuel cells are important to reduce the need of fossil fuels and to decrease/eliminate hazardous emissions caused by burning fossil fuels (Carrette *et al.*, 2001).

A fuel cell is an electrochemical tool attaining electrical energy from the chemical energy of a fuel. This one-step process has a clean and efficient mechanism that is suitable to use hydrogen as fuel instead of traditional fossil fuels. This nature of the FC technology takes a substantial role in sustainable energy concern of the world in addition to its advantage of being cleaner, more efficient and more flexible. A fuel cell consists of an anode, a cathode, and an electrolyte membrane between them (Sharaf and Orhan, 2014).

There are several types of FCs, such as proton exchange membrane fuel cells (PEMFCs), alkaline fuel cells (AFCs), direct methanol fuel cells (DMFCs), phosphoric acid fuel cells (PAFCs), molten carbonate fuel cells (MCFCs), and solid oxide fuel cells (SOFCs). Fuel option, operating temperature and electrolyte material can differ for types of FCs and the most promising FC technology for transport and small-scale applications is the PEMFC type (Trimm and Önsan, 2001). A PEMFC has low operating temperatures, below 90 °C and mostly at around 80 °C, and uses platinum catalyst which is highly sensitive to CO existence.

In a typical PEMFC, hydrogen ions and electrons are produced from a hydrogen molecule at the anode of the FC, shown as Equation 2.1. These hydrogen ions and electrons react with oxygen molecule to yield water at the cathode, shown as Equation 2.2. Overall, water, electrical power and heat are generated from hydrogen and oxygen molecules in the fuel cell in the form of Equation 2.3 (Sharaf and Orhan, 2014).

$$H_2 \rightarrow 2H^+ + 2e^- \quad (2.1)$$

$$\frac{1}{2}O_2 + 2H^+ + 2e^- \rightarrow H_2O \quad (2.2)$$

$$H_2 + \frac{1}{2}O_2 \rightarrow H_2O + W_{electrical} + Q_{heat} \quad (2.3)$$

2.2. Fuel Processors and Reactions

Hydrogen is the most promising fuel option for FCs thanks to its safe, efficient and environment-friendly nature in the process. However, unfortunately, storing hydrogen and directly using it in a PEMFC for small scale applications is not reasonable because of its high volume requirement. To overcome this problem, a fuel processor (FP) is constructed to obtain hydrogen which is especially CO free since it is fed to a PEMFC whose Pt-based catalyst is poisoned by CO concentrations higher than 100 ppm (Tiwari *et al.*, 2014). When fuel types are considered, gasoline and diesel are studied and used for on-board or mobile application since they have well-established distribution network for vehicles. On the other hand, natural gas mainly consisting of methane and LPG mainly consisting of propane are the preferred fuel options of a fuel processor for on-site or small scale stationary applications such as household usage. Particularly natural gas option which is commonly used in houses is preferable thanks to its well established pipeline system at the present time.

A FP is a combination of a hydrogen-producing unit and one or more CO-cleaning unit(s). Main purpose of a FP is to produce H_2, for FCs or any other equipment utilizing H_2. Since fuel cell type is chosen as PEMFC, the H_2 fuel produced by a FP should be CO-free, or at least with CO concentration lower than 100 ppm, more preferably lower than 40 ppm. Therefore, there is a special need to place CO-cleaning unit after a H_2-producing unit. Reforming unit which mainly produces H_2 is the first unit a FP but significant amount of CO is generated at this unit, as well. Since CO concentration should be decreased below a certain limit, there should be CO-cleaning units after a reforming unit. For that purpose, a water-gas-shift (WGS) unit exists to reduce CO content in the product stream of reforming unit. As WGS enhancement in a FP, high- and low-temperature-shift units (HTS and LTS) or a

single WGS unit operating at an intermediate temperature can be used. For further CO cleaning, if necessary, preferential (or selective) oxidation (PROX) unit or selective CO-consuming methanation unit is placed (Başar, 2016). To understand mechanism of a FP, reactions in reforming unit, WGS unit and PROX unit are broadly explained in Sections 2.2.1, 2.2.2 and 2.2.3, respectively.

2.2.1. Reforming Reactions

Reforming process is a well-known and established technology for H_2 production, especially in petroleum industry. The options of reforming reactions for a FP are steam reforming (SR), partial oxidation (POX) and oxidative steam reforming (OSR). CO producing SR reaction and CO_2 producing SR reaction are shown in Equation 2.4 and Equation 2.5, respectively. Although SR reactions yield high-concentration-H_2, their excessive need for heat due to their high endothermicity is the main drawback. POX which is another way to produce hydrogen, is shown in Equation 2.6 whereas total oxidation (TOX) which is a side reaction in terms of hydrogen production is shown in Equation 2.7. Ni based catalysts are conventionally used for industrial purposes even though Ni is less active compared to certain noble metals. (Welaya *et al.*, 2012).

$$C_mH_{2n} + mH_2O \leftrightarrow mCO + (m+n)H_2 \qquad \Delta H > 0 \qquad (2.4)$$

$$C_mH_{2n} + 2mH_2O \leftrightarrow mCO_2 + (2m+n)H_2 \qquad \Delta H > 0 \qquad (2.5)$$

$$C_mH_{2n} + \left(\frac{1}{2}m\right)O_2 \rightarrow mCO + nH_2 \qquad \Delta H < 0 \qquad (2.6)$$

$$C_mH_{2n} + \left(m + \frac{1}{2}n\right)O_2 \rightarrow mCO_2 + nH_2O \qquad \Delta H < 0 \qquad (2.7)$$

On the other hand, OSR is a combination of steam reforming and partial oxidation and the overall reaction is shown as Equation 2.9. The idea behind is that exothermicity of oxidation reaction provides necessary heat for endothermic steam reforming reaction. By adjusting feed ratios of steam and oxygen, whole system can be energetically balanced, i.e.

there will be no need of external heat supply for the whole system if steam and oxygen ratios is properly arranged. This special case of oxidative steam reforming is known as autothermal reforming (ATR) (Palma *et al.*, 2017).

$$CH_4 + xO_2 + yH_2O \leftrightarrow aCO + bCO_2 + cCH_4 + dH_2O + eH_2 + fC_{(s)} \qquad (2.9)$$

High endothermicity of SR reactions is the main reason to couple them with exothermic oxidation reactions to be able to operate at lower temperatures. Oxygen amount is the key point since excess oxygen is used more rapidly in oxidation reactions than SR reactions. Oxygen and steam amounts at the feed are important for performance and product stream composition a reformer unit/FP system (Erdinç, 2014). When methane is taken as the fuel for reforming reactions in a FP, like in this study, reactions taken into consideration are listed in Equation 2.10-15. Methanation reactions listed in Equation 2.14 and 2.15 are the reverse forms of SR reactions (Welaya *et al.*, 2012; Başar, 2016).

$$CH_4 + H_2O \rightarrow CO + 3H_2 \qquad \Delta H^{\circ}_{25^{\circ}C} = 206\ kJ/mol \qquad (2.10)$$

$$CH_4 + 2H_2O \rightarrow CO_2 + 4H_2 \qquad \Delta H^{\circ}_{25^{\circ}C} = 165\ kJ/mol \qquad (2.11)$$

$$CH_4 + \frac{1}{2}O_2 \rightarrow CO + 2H_2 \qquad \Delta H^{\circ}_{25^{\circ}C} = -38\ kJ/mol \qquad (2.12)$$

$$CH_4 + 2O_2 \rightarrow CO_2 + 2H_2O \qquad \Delta H^{\circ}_{25^{\circ}C} = -803\ kJ/mol \qquad (2.13)$$

$$CO + 3H_2 \rightarrow CH_4 + H_2O \qquad \Delta H^{\circ}_{25^{\circ}C} = -206\ kJ/mol \qquad (2.14)$$

$$CO_2 + 4H_2 \rightarrow CH_4 + 2H_2O \qquad \Delta H^{\circ}_{25^{\circ}C} = -165\ kJ/mol \qquad (2.15)$$

2.2.2. Water-Gas Shift Reaction, WGS

WGS is a fundamental step for hydrogen production methods since it is a reaction consuming CO and H_2O to produce CO_2 and H_2, as shown in Equation 2.16. WGS not only consumes CO to clean a product stream of a reforming unit/hydrogen producing unit but

also generates additional hydrogen. It is has a unique and important role in a FP system with the help of this characteristic (Mandapaka and Madras, 2017).

$$CO + H_2O \leftrightarrow CO_2 + H_2 \qquad \Delta H^{\circ}_{25^{\circ}C} = -41.2\ kJ/mol \qquad (2.16)$$

WGS is a mildly-exothermic thermal equilibrium reaction and it is reversible. Even though thermal equilibrium conversion limit is decreased with increasing temperature, WGS reaches equilibrium faster at high temperatures. On the other hand, WGS at low temperatures is also attractive since its thermal equilibrium conversion is higher at low temperatures, despite low kinetics. In a nutshell, WGS is thermodynamically limited at high temperature, and kinetically limited at low temperatures. Therefore, conventional WGS operation is divided into two reactors which are HTS and LTS reactors (LeValley *et al.*, 2014).

HTS reactor is operated at 350-600 °C to speed up the reaction kinetically and iron/chromium based catalyst are conventionally used in industry for this reaction. On the other hand, copper/zinc based catalyst are used for LTS reactor which is operated at 150-300 °C (Tiwari *et al.*, 2014). But these Fe-Cr and Cu-Zn based catalysts are pyrophoric, which is not usable in air/O_2-containing environment, and therefore they are not suitable for a FP system producing H_2 via OSR since oxygen and steam exist in the system. Consequently, two-step WGS process is not viable for small scale application such as FP, and the inapplicability of pyrophoric catalyst leads to research of new catalyst for a single step WGS unit operating at intermediate temperatures. Noble metals (such as Pt, Au etc.) supported on ceria, zirconia, alumina etc. are studied for WGS unit for the need of non-pyrophoric, poison resistant and thermally stable, noble metal based WGS catalysts (Çağlayan and Aksoylu 2009; Çağlayan and Aksoylu 2011a; Tiwari *et al.*, 2014; LeValley *et al.*, 2014).

2.2.3. Preferential Oxidation Reaction, PROX

Since CO removal of product stream of a reforming unit in a FP system via WGS unit is not enough in terms of reducing CO concentration below 100 ppm, more preferably below 40 ppm, an additional CO-cleaning unit is desired. PROX and selective methanation technics are the options for selective CO removal but PROX unit is preferable since selective

methanation of CO directly consumes valuable H_2 product. Therefore, a PROX unit follows a WGS unit in a FP system to decrease CO concentration, and CO oxidation reaction is shown in Equation 2.17. In addition to this reaction, undesired hydrogen oxidation is unavoidable, as shown in Equation 2.18 (Ashraf *et al.*, 2014).

$$CO + \frac{1}{2}\,O_2 \rightarrow CO_2 \qquad \Delta H^{\circ}_{25^{\circ}C} = -283\ kJ/mol \qquad (2.17)$$

$$H_2 + \frac{1}{2}O_2 \rightarrow H_2O \qquad \Delta H^{\circ}_{25^{\circ}C} = -242\ kJ/mol \qquad (2.18)$$

Noble metals like gold, copper and platinum on supports such as alumina, iron-oxide and ceria have been studied in the literature (Romero-Sarria *et al.*, 2016). Pt is one of the best active metals for PROX reaction and other supports like zeolite and activated carbon (AC) are also investigated. For a PROX unit which is one the units in a FP system, a PROX catalyst should work in the presence of H_2O, H_2, CO_2 in addition to CO and O_2. In this concept, Pt-Sn based catalyst supported by AC were studied by our group (Şimşek *et al.*, 2007; Çağlayan *et al.*, 2011b; Eropak and Aksoylu, 2017). PROX is operated generally at 100-130 °C range, even lower than 120°C, since the reaction in PROX unit are highly exothermic.

2.3. Complete FP Systems Using Methane/Natural Gas as Fuel

Cipiti *et al.* investigated a methane fuel processor consisting of an ATR unit, a CO shift converter (WGS unit), a PROX unit and internal heat exchangers to produce hydrogen for a polymer electrolyte fuel cell in residential usage. Pt/CeO_2 (proprietary), Pt/CeO_2-ZrO_2 (commercial) and Ru/Al_2O_3 (commercial) were used as catalysts and operating temperatures are 700 °C, 350 °C and 120 °C (light-off temperatures of 450 °C, 250 °C and 90 °C) for ATR, WGS and PROX units, respectively. Via continuous test for a total of 1000 h with daily cycles of 6 h, start-up, regime (steady state) and shut-down phases were observed. 20 min of start-up period was achieved and 5.0 Nm^3/h of hydrogen production resulted in stable operation temperatures for three units. Moreover, this nominal 5.0 Nm^3/h of hydrogen production provided good stability with 37% methane conversion in the absence of carbon deposition. CO concentration in the effluent stream of PROX unit was negligible, close to 0

ppm, for hydrogen productivity of 5.0 Nm^3/h. Besides, heat balances for each unit were reported and shut-down period was observed as ca. 4 h, i.e. temperatures of all units approximately approached to ambient temperature in 4 h. Relatively long start-up time, non-perfect homogenization of the temperatures, hot spots, lack of flexibility in regime phase, difficulty of thermal integration were main problems of the system and performance of the system was reported as extremely sensitive to production level (Cipiti *et al.*, 2013).

Another fuel processor system using ATR of natural gas to produce hydrogen in kW scale was studied by Palma *et al.* The system consisted of a mixer, an ATR unit, a compact heat exchanger and a WGS unit, sequentially. Thanks to the heat exchanger heating reactants with effluent stream of ATR unit, thermal integration was achieved and a good heat recovery was obtained through this configuration. ATR and WGS units were cylindrical reactors and commercial noble metal based honeycomb monolith catalyst (Johnson Matthey) and commercial pellet $Katalco_{JM}$ 74-5M catalyst were used in ATR and WGS units, respectively. Both 99.5% pure methane and natural gas were used as reactant whereas and O_2/fuel ratio of 0.55-0.65, H_2O/fuel ratio of 0.6-1.00, gas hourly space velocity (GHSV) of reactants of 15,000-22,500 h^{-1} were tested in this study at atmospheric pressure. As conclusion in the study, a good performance of ATR despite thermal integration and changing feed ratios was obtained while WGS performance was not adequate due to commercial catalyst usage. Up to 10 Nm^3/h of hydrogen was produced and thermal efficiency of 65% was obtained and reported as higher than previous works in the literature, in the case of natural gas feed. However, final CO concentration in the exit of WGS unit altered in 4-8% which is too high for a PEMFC system (Palma *et al.*, 2017).

Connected to full fuel processor system, Palma *et al.* also studied an intensification of methane steam reforming. In this study, experimental work was done and preliminary steady-state 3D model was constructed. Silicon Carbide monoliths was used as catalyst support for Ni loading thanks to their high thermal conductivity. Two different flow configurations which were Flow Through (FT) and Wall Flow (WF) were studied. Activity of WF configuration was better than FT in terms of hydrogen yield. Experimental results agreed with numerical modelling results and WF configuration enhanced hydrogen production in which mass and energy limitations existed (Palma *et al.*, 2016).

Another fully constructed and modelled fuel processor system was studied by Jung *et al.* This fuel processor had a burner, a steam reformer, a WGS unit and a PROX unit, sequentially. Instead of ATR, there were a separate burner where some part of natural gas feed was oxidized to heat up the system and then a methane steam reformer unit whose catalyst and operating temperature were Ru(2.0)/Al_2O_3 and 680-700 °C, respectively. After reformer, WGS unit whose catalyst and operating temperature were Pt(2.0)/ZrO_2 and 180-330 °C, respectively, and then PROX unit whose catalyst and operating temperature were Ru(0.5)/Al_2O_3 and 100-150 °C, respectively, existed. Parametric studies on temperature at the exit of the reformer and percent load were done and corresponding product gas compositions and thermal efficiencies were reported. In all cases, PROX exit CO concentration on dry basis was less than 5 ppm, and overall thermal efficiency was ca. 80% (Jung *et al.*, 2014).

For the systems producing hydrogen with CO content or sole reformer units can be upgraded by addition of CO clean up systems consisting of WGS and/or PROX units (O'Connell *et al.*, 2010; Ashraf *et al.*, 2014). O'Connell *et al.* developed a microstructured combined WGS and PROX unit to clean up a diesel refomate unit in the 5 kW range. They used feed streams containig 8.8 vol% CO (wet base) and 0.7 vol% CO (wet base) for WGS and PROX units, respectively. Conversion of CO in WGS unit was 95% and CO concentration decreased to 0.78 vol% at the exit of WGS whereas conversion of CO in PROX unit was 99.75% and exit concentration of PROX was 25 ppm (O'Connell *et al.*, 2010). On the othar hand, Ashraf *et al.* simulated and compared autothermal reforming with steam reforming and CO-PROX with CO selective methanation (SMET) in four combinations which all had WGS unit. They conclude that there was not any significant advantage of autothermal reformer and CO-PROX unit over steam reforming and CO-SMET, respectively. Due to complexity and relatively highr cost of autothermal reformer and CO-PROX, steam reformer and CO-SMET unit could be replaced, as a trade-off between performance and complexity/cost (Ashraf *et al.*, 2014).

2.4. Individual OSR Units of FP Systems

2.4.1. Fuels for OSR Units

Beside complete fuel processor systems producing CO-free hydrogen for a PEMFC, only reformer parts of fuel processors, without CO clean up like WGS or PROX unit, are commonly studied in the literature. These can be separate studies or these studies, e.g. the paper written by Ni *et al.*, are to produce hydrogen containing CO for fuel cells which are resistant to CO existence like solid oxide fuel cells. Ni *et al.* studied an integrated natural gas fuel processor using a steam reforming and a separate heater with a catalyst of $Rh/MgO/Ce_{0.5}Zr_{0.5}O_2/Al_2O_3$, for 2-kW solid oxide fuel cell. They integrated also two separate heat exchangers to heat up fresh feed streams via effluent stream of the reformer unit. Conversion levels increased with increasing reformer temperature in the range of 700-840 °C and were close to 100% at higher temperatures. Thermal efficiency was ca. 74% at most in the hydrogen production of $2Nm^3/h$. Moreover, they investigated start-up and shut-down periods, and the system was stable during 5 different start-up periods (Ni *et al.*, 2015).

In addition to natural gas/methane, LPG/propane is also used for small scale stationary applications. Malaibari *et al.* studied oxidative steam reforming of LPG on Mo-15 wt.% Ni/Al_2O_3 catalyst. Their LPG feed consisted of 1:1 propane-butane and effect of Mo loadings of 0.05, 0.1, 0.3 and 0.5 wt.% were investigated. In the reaction conditions of 450 °C, steam to carbon of 3 and oxygen to carbon of 0.3, lowest Mo loading, which was 0.05 %, had the best activity and stability compared to other loadings of Mo and only Ni loading. Moreover, oxidative steam reforming was compared with steam reforming via running additional steam reforming experiments. They concluded that Mo loading decreased carbon deposition on the catalyst and oxidative steam reforming decreased it to zero. Consequently, 0.1wt.% Mo-15wt.% Ni/Al_2O_3 was found as active and stable with a conversion of 88% and a H_2 production rate of 80×10^{-5} mol/min (Malaibari *et al.*, 2014).

When mobile applications are considered, different feeds than natural gas and LPG like methanol, ethanol, gasoline, diesel etc. are used in fuel processors. For instance, Yang *et al.* developed a self-sustained methanol fuel processor producing 1 m^3/h H_2 with CO concentration below 25 ppm. Its thermal efficiency was at most 86% and start-up time was

ca. 10 min (Yang *et al.*, 2015). On the other hand, Gardemann *et al.* designed and demonstrated an ethanol fuel processor consisting of a reformer, a WGS unit, a catalytic burner and heat exchangers for high temperature PEMFC with 200-500 W. Start-up time was less than 30 min and efficiency was 55% but CO percentage at the exit was 1-1.5% which was acceptable for a high temperature PEMFC but too high for common PEMFC systems (Gardemann *et al.*, 2014).

Methanol and less toxic ethanol are preferred fuel options for portable applications such as military, leisure and security power supplies whereas gasoline and diesel are attractive feed options for power supply and vehicle applications. Ji *et al.* studied and tested a gasoline fuel porcessor consisting of an ATR unit, two WGS units (high- and medium-temperatured), a PROX unit, a heat exchanger and an external burner. First, the burner was ignited, then the PROX unit started and lastly the reformer unit operated. Via this start-up strategy a reformate stream containing >40 vol.% H_2 and <0.5 vol.% CO within 30-35 min was obtained (Ji *et al.*, 2015). In another study, diesel was used as feed of reforming unit in a fuel processor-fuel cell combined system by Samsun *et al.* They investigated petroleum-based and synthetic-based diesel, and kerosene fuels for fuel processor-fuel cell system producing 28 kW thermal power for trucks and aircrafts. Their system consisted of an autothermal reformer, a WGS unit and a catalytic burner. Simulation and experimental results were compared and both PEMFC and high temperature PEMFC are used where CO concentration at the exit is 1.5-5.1 vol.% (Samsun *et al.*, 2015).

2.4.2. Analyses of Individual OSR Units

For a OSR unit, temperature and feed conditions (steam-to-carbon, oxygen-to-carbon ratios) are important parameters to be examined. Sepehri and Rezaei studied effects of these parameters on methane ATR, which is a special case of OSR, in addition to Ce promoting effect on the activity of Ni/Al_2O_3 catalyst. Moreover, gas hourly space velocity (GHSV) was investigated to understand its effect on the performance. They showed that methane conversion of ATR was increased with rising temperature. Similarly, S/C and O/C ratios of the feed for ATR had a positive effect on methane conversion of ATR in their study, i.e. methane conversion was raised with increasing any of S/C and O/C ratios. Their study stated that GHSV had a lower impact on conversion but still the effect of GHSV on methane

conversion was signficant and methane conversion decreased with increasing GHSV. Moreover, they indicated that small amount of ceria addition to Ni/Al_2O_3 catalyst had a significant effect on the performance of ATR. 3 wt.% Ce loading among 1, 3 and 6 wt.% Ce loadings had the best improvement on methane conversion and stability of ATR performance (Sepehri and Rezaei, 2017).

There are other studies investigating effects of different additions to conventional Ni based reforming catalysts. For instance, Dias and Assaf studied the enhancement of adding small quantities of noble metals into $Ni/\gamma\text{-}Al_2O_3$ catalyst for ATR of methane. They examined Pt, Pd and Ir additions which were less than 0.3% by weight into $15\%Ni/\gamma\text{-}Al_2O_3$ catalyst. Increased methane converison in ATR was observed with the additions of noble metals. The enhancement in methane conversion was caused by increased metal surface area, even though there was not any electronic modification of nickel sites due to the addition of noble metals. They found a proportional rise in methane conversion with the raise in metal surface area (Dias and Assaf, 2004).

Changjun *et al.* studied $Ce\text{-}ZrO_x$, $Ce\text{-}LaO_x$, $Ce\text{-}SmO_x$ and $Ce\text{-}GdO_x$ additions to Rh/Al_2O_3 catalysts for use in a methane ATR system. Among the used Ce-metal oxides, $Ce\text{-}ZrO_x$ was the best in terms of reducing concentration of CO in the effluent stream. Besides, Ce/Zr atomic ratio was investigated to find which ratio is appropriate for a stable catalyst and the ratio of 1:1 resulting $Ce_{0.5}Zr_{0.5}O_2$ was found as the most stable addition to the catalyst. Moreover, the effects of doping different alkaline earth metals on the most stable catalyst were examined. Among Mg, K and Ca, Mg doping in oxide form of MgO was the best to provide carbon resistance to the catalyst. The resulting and optimized catalyst was $0.1\%Rh/2.0\%MgO/40\%Ce_{0.5}Zr_{0.5}O_2/Al_2O_3$ (Ni *et al.*, 2014).

OSR reactions, consisting of SR and POX with other undesired reactions including TOX, are also tested on microchannel/monolith reactors, especially to examine space/contact time effect since POX/TOX reactions are known for their dependencies on contact time. Şimşek *et al.* studied an OSR of methane system to produce syngas over alumina supported bimetallic Pt-Rh catalyst in both microchannel and packed-microchannel reactors. They investigated effects of temperature, steam-to-carbon and oxygen-to-carbon ratios, and contact time and stated that increase in all parameters resulted in enhancement in

methane conversion. They used short contact times and so there were thermodynamic limits for methane conversion. The results were discussed in favor of syngas production but still the study had a considerable importance on understanding the performance of a methane OSR system (Şimşek *et al.*, 2013).

Another performance analysis of a methane OSR system was studied by Vita *et al.* 1.5 wt.% $Ru/\gamma\text{-}Al_2O_3$ catalyst on a monolith reactor was prepared and its surface was investigated by techniques of X-ray Diffraction, N_2 adsorption, H_2 chemisorption, SEM analysis and mechanical strength tests. Three monoliths with three different catalyst loads were prepared and the best one was determined and used to examine the effects of temperature, O/C and S/C ratios and weight space velocity (WSV) on the performance of OSR. They stated that temperature had a significant positive effect on methane conversion whereas O/C and S/C ratios did not have a remarkable effect on methane conversion, but affected the product distribution of OSR on a limited basis. Furthermore, WSV effect was shown as almost insignificant for methane conversion and product distribution in their testing range, especially over a WSV of 100,000 N ml $g_{cat}^{-1}h^{-1}$ (Vita *et al.*, 2014).

Vita *et al.* also studied syngas production by methane OSR over metal-loaded ceria catalyst on monolith reactors using Rh, Pt, and Ni as active metals. Again, this is a study focusing on syngas production which has short contact times to prevent further oxidation of methane (TOX) and to favor POX for higher CO concentration but it is still informative about methane OSR characteristics. In parallel with previous study of Vita el al., explained in previous prapraph above, they tested structured catalysts for methane OSR on monolith reactors at constant O/C ratio of 0.55 and S/C ratio of 1.2 to investigate the effects of temperature and WSV on the performance of methane OSR. While increasing temperature, methane conversion of OSR was raised with rising H_2 and CO percentages in the product for all of metal loadings. On the other hand, they stated that WVS increase resulted in a negligible methane conversion loss for Rh/CeO_2 and Pt/CeO_2 catalysts, but a significant reduction in methane conversion for Ni/CeO_2 catalyst. As the result of active metal comparison, Rh was the best metal for methane OSR performance with very similar performance of Pt whereas Ni was remarkably worse than those in terms of performance (Vita *et al.*, 2015).

For a single reaction, it is expected that conversion is risen with an increase in residence/contact/space time or a decrease in space velocity since reactants will have more time to react. Residence time effects for propane OSR in metallic microchannel reactors were examined by Aartun *et al.* They studied Rh-impregnated microchannel reactors in POX or OSR for hydrogen or syngas production. The mettallic microchannel reactor was found as capable of minimizing temperature gradients along the reactor. They stated that H2 formation in OSR was higher as compared to POX, with the help of WGS reaction existence in OSR. Residence time vs. propane coversion graphs were provided by Aartun *et al.* and it was seen that up to a specific residence time, ca. 25 ms, propane conversion was increased than stayed approximately constant. However, further increase in residence time resulted in a small decrease in propane conversion as shown in Figure 2.1 (Aartun *et al.*, 2005). It was not a concern in the paper but this behavior is questionable and worth to consider if further increase in residence time will cause a sharper decline in the conversion.

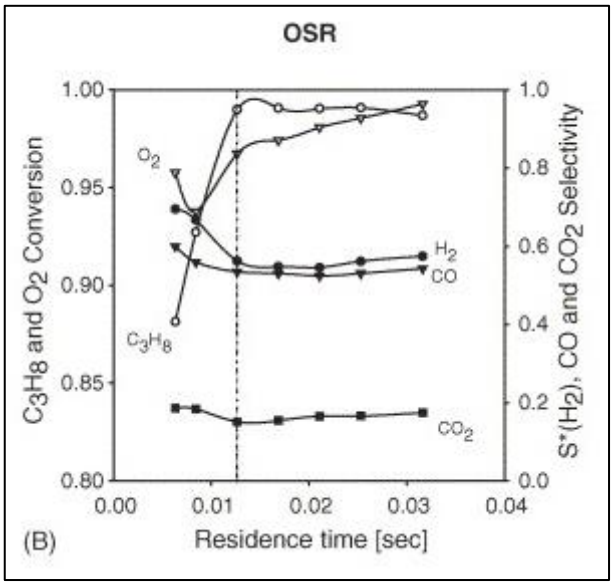

Figure 2.1. Conversion and selectivity vs. residence time graph of Aartun *et al.* (Aartun *et al.*, 2005).

Another study examining space time effect on methane conversion of an OSR system was done by Ryu *et al.* They used small amounts of Ru or Pt doped commercial Ni catalyst in the form of powdered catalyst and as wash-coated on metal monolith reactor. Methane conversion in monolith reactor was found as higher compared to powdered catalyst

containing reactor. It was shown in the paper that increase in gas hourly space velocity (GHSV) had a negligible effect on methane conversion up to a certain value, different value for different forms of the catalyst, and a significant effect decreasing methane conversion above that value. This was a usual trend, however; there was an extraordinary result indicating that a rise in GHSV yield in a remarkable raise in methane conversion at a low GHSV value of the operation range as shown in Figure 2.2 (Ryu *et al.*, 2007). Similar to the last paper explained in previous paragraph just above, that evokes a question about how space velocity affects methane conversion of a OSR system.

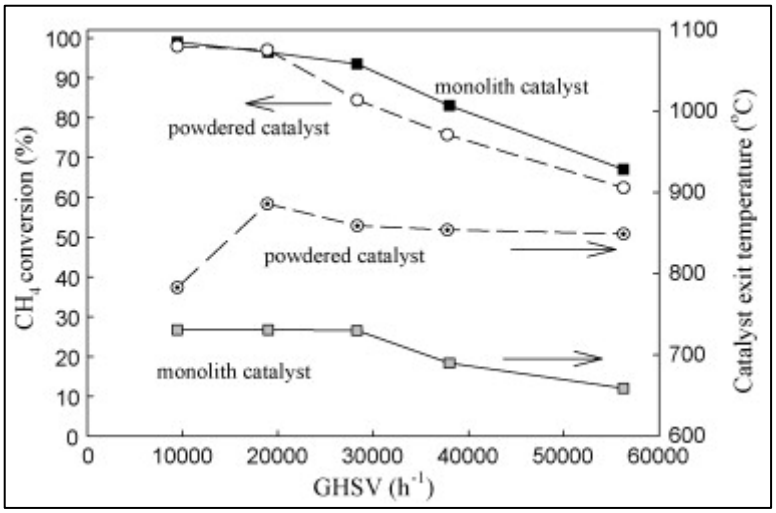

Figure 2.2. Conversion and temperature vs. GHSV graph of Ryu *et al.* (Ryu *et al.*, 2007).

7.5 wt.%Ni-CeO_2 catalysts were prepared by different methods and used to investigate which method led to the best activity in biogas, biomethane, OSR system at specifed temperature, S/C and O/C ratios with varying weight space velocity (WSV) by Balzarotti *et al.* Constructed catalysts were characterized by XRD, BET, CO-Chemisorption, TPR, TEM and SEM-EDX techniques. The study indicated that methane conversion decreased with increasing WSV at all WSV values in the range, except the WSV values of 30,000-70,000 $Nmlg_{cat}^{-1}h^{-1}$. Between these values of WSV, a rise in WSV yielded an increase in methane conversion instead of a fall, as shown in Figure 2.3 (Balzarotti *et al.*, 2016). That was not a concern in the related article, but again it is important to recognize for further analyses of space velocity effect on OSR systems.

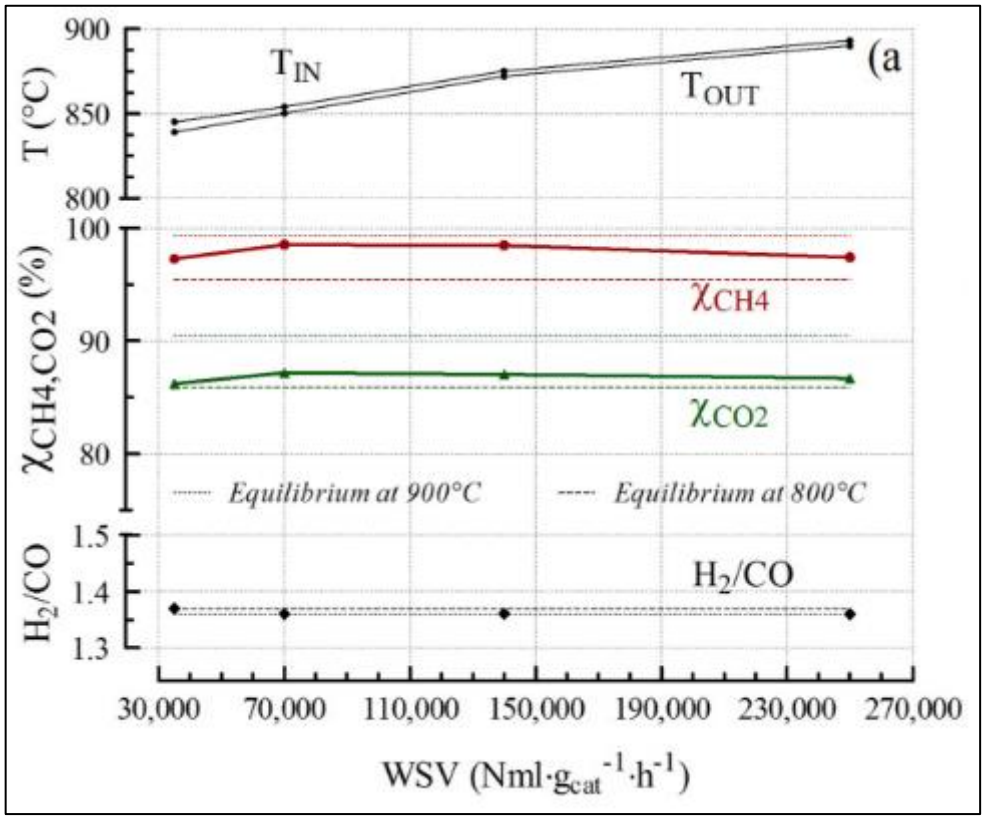

Figure 2.3. H_2/CO ratio, conversion and temperature vs. WSV graph of Balzarotti *et al.* (Balzarotti *et al.*, 2016).

Besides performance analyses of OSR/ATR units, there are several thermodynamic analyses for those systems. Souza *et al.* did a thermodynamic analysis for a methane ATR system via maximazing entropy method. A wide range of steam-to-methane ratio (S/M), oxygen-to-methane ratio (O/M), inlet temperature and system pressure were examined to reach equilibrium conditions via entropy maximization in the article. Optimum O/M ratio at 1 bar, methane conversion, hydrogen yield, CO and coke formations etc. were calculated by nonlinear programming in GAMS®, using CONOPT2 solver. Moles of hydrogen produced, moles of coke formed, conversion percentage reached, etc. were demonstrated per inlet mole of methane in varying S/M and O/M ratios. The results indicated that coke formatino was negligible at S/M ratios higher than 1.5 and methane conversion is directly proportional to S/M and O/M ratios when S/M ratio is above 2. Moreover, it was stated that low pressure and high S/M ratios favored hydrogen production and the maximum hyrogen amount was achieved at S/M = 5 and O/M = 0.18 (Souza *et al.*, 2014).

Zeng *et al.*, studied a system producing hydrogen from propane OSR to make a thermodynamic analysis with a Gibbs free energy minimization method by using HSC Chemistry 4.0 programme. Equilibrium compositions were found in changing temperature, steam-to-propane and oxygen-to-propane ratios under oxidative and thermo-neutral, i.e. ATR, conditions. They demonstrated H_2, CO, and CH_4 yields and coke formation as a function of steam-to-propane and oxygen-to-propane ratios. Furthermore, thermo-neutral temperature were determined as 700 °C at atmospheric pressure and steam-to-propane ratio of 7.0-13.0 was found as appropriate for high hydrgoen and low carbon monoxide yield in propane OSR sytem (Zeng *et al.*, 2010).

Another thermodynamic analysis of a hydrogen producing system was made on a methanol OSR reactor via a Gibbs free energy minimization method with a commercial software Outokumpu HSC Chemistry 4.0 by Wang *et al.* The equilibrium yields of H_2, CO, CH_4 and coke were obtained as a function of steam-to-methanol ratio, oxygen-to-methanol ratio and temperature. At lower temperatures, methane was found as the main product whereas increasing temperature caused main products of hydrogen and carbon monoxide. Increasing steam-to-methanol ratio led to favoring H_2 production while inhibiting CO, CH_4 and coke formations. Rise in oxygen-to-methanol ratio provided energy for OSR and prevented coke formation, but further raise favored undesired TOX of methanol. High steam-to-methanol ratio, low oxygen-to-methanol and relatively high temperature resulted in the best performance of methanol OSR in terms of producing hydrogen (Wang *et al.*, 2012).

3. EXPERIMENTAL WORK

3.1. Materials

3.1.1. Chemicals

All chemicals used for catalyst preparation in this research are research grade with high purity and they are listed in Table 3.1.

Table 3.1. Chemicals used for catalyst preparation.

Chemical	Formula	Specification	Source	MW (g/gmol)
Aluminum oxide	γ-Al_2O_3	Catalyst support, high surface area	Alfa Aesar	101.96
Nickel (II) nitrate hexahydrate	$Ni(NO_3)_2.6H_2O$	99+%	Merck	290.81
Tetraammine platinum (II) nitrate	$Pt(NH_3)_4(NO_3)_2$	99.995%	Sigma-Aldrich	387.22

3.1.2. Gases and Liquids

Formula, specification and application information of gases used in this research is listed in Table 3.2. All of the gases listed were supplied by the Linde Group, Gebze, Turkey. The only liquid used in this research is deionized water. Formula, specification and application information of water is listed in Table 3.3.

Table 3.2. Specifications and applications of the gases used.

Gas	Formula	Specification	Application
Carbon dioxide	CO_2	99.995%	MS calibration
Carbon monoxide	CO	99.998%	MS calibration
Helium	He	99.999%	MS calibration/Inert
Hydrogen	H_2	99.998%	MS calibration/Reducing agent
Methane	CH_4	99.5%	MS calibration/Reactant
Oxygen	O_2	99.998%	MS calibration/Reactant

Table 3.3. Specification and application of the liquid used.

Liquid	Formula	Specification	Application
Water	H_2O	Deionized (DI)	Aqueous solutions, Reactant

3.2. Experimental Systems

The current experimental systems are composed of mainly two parts which are catalyst preparation system and catalytic reaction system.

3.2.1. Catalyst Preparation Systems

The system shown in Figure 3.1 is used for catalyst preparation by incipient-to-wetness impregnation technique and consists of a Retsch UR1 ultrasonic mixer, a Büchner flask, a KNF Neuberger vacuum pump, a Masterflex peristaltic pump, a beaker containing the precursor solution and a silicon tubing.

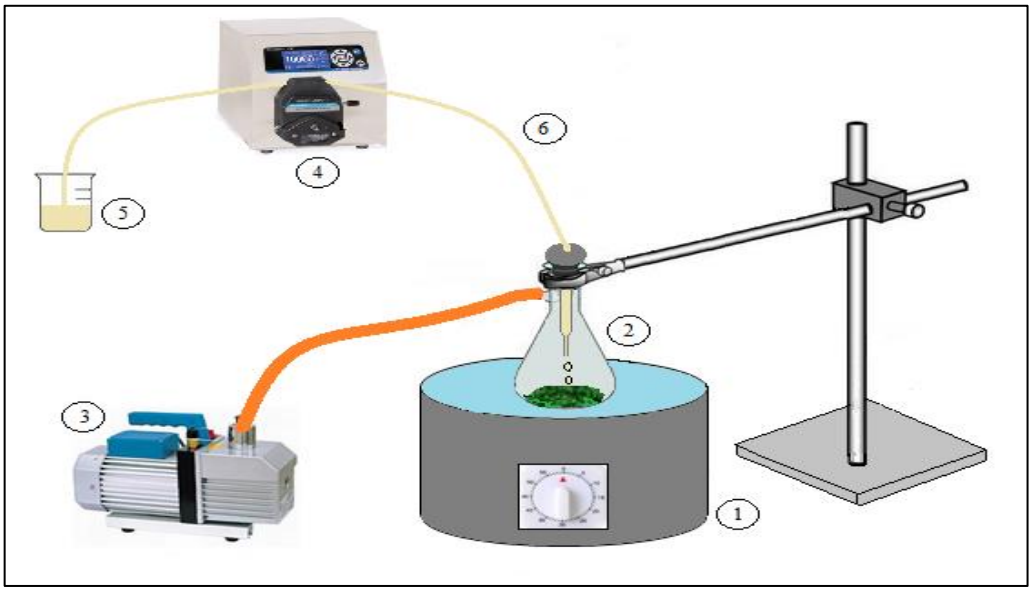

Figure 3.1. Schematic diagram of the impregnation system:
1. Ultrasonic mixer, 2. Büchner flask, 3. Vacuum pump, 4. Peristaltic pump, 5. Beaker, 6. Silicone tubing (Başar, 2016).

According to this method, a specific amount of catalyst is placed in the Büchner flask to evacuate air in pores of the support, before impregnation procedure. For this purpose, support in the Büchner flask is mixed for 30 minutes by a Retsch UR1 ultrasonic mixer under vacuum provided via a KNF Neuberger vacuum pump. This operation makes support pores more available in terms of metal penetration in the pores during impregnation. Afterwards, pre-prepared precursor solution is fed through a silicone tubing onto the support in the Büchner flask via a Masterflex computerized-drive peristaltic pump with a flow rate of 0.5 ml/min. This wet-support as a slurry is mixed in the ultrasonic mixer during impregnation to ensure a better precursor distribution and a uniform metal dispersion on the support surface. After the impregnation, the slurry is mixed by the ultrasonic mixer for another 90 minutes under vacuum. The thick slurry obtained at the end of the procedure is dried overnight in the oven in order to remove remaining water content.

3.2.2. Catalytic Reaction System

The pre-constructed Fuel Processor Prototype (FPP) system, shown in Figure 3.2, is composed of three sections which are feed, reaction and analysis sections.

The FPP is constructed and configured for OSR-WGS-PROX serial experiments but in this study, only one reactor is used for performance analysis of OSR of the FPP system.

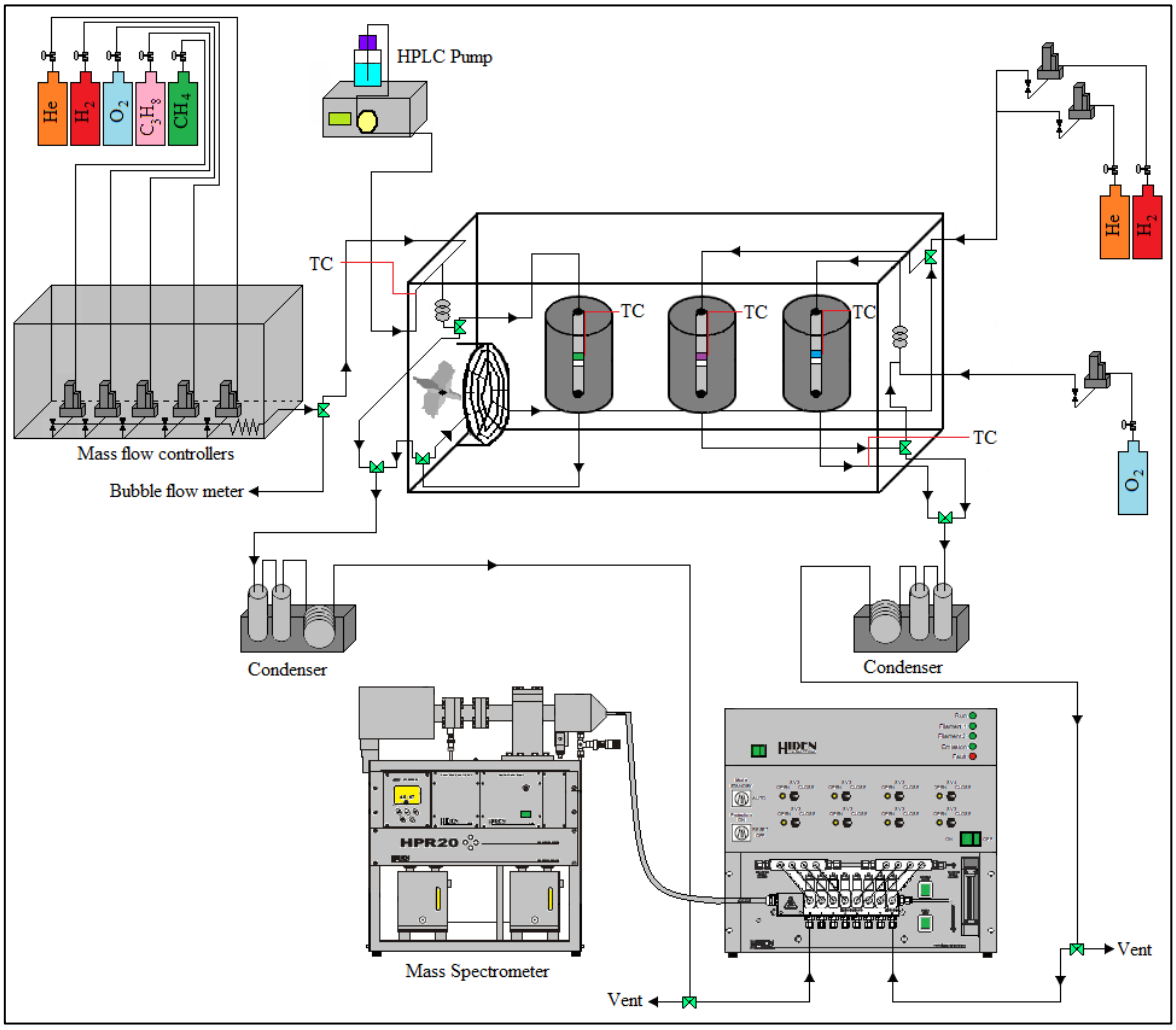

Figure 3.2. Schematic diagram of the FPP (Başar, 2016).

The feed section of the FPP system contains Brooks model 5850E mass flow controllers (MFCs) for the inlet gases, a Jasco PU-2089 Plus HPLC pump for the water inlet and stainless steel (SS) tubing, valves and fittings. Each gas is fed through a separate line via an MFC and an on-off valve is placed for each MFC to protect MFCs against a possibility of back pressure. Water feeding line is in the form of a 1/16'' SS tubing and its temperature is kept at 140 °C via a Shimaden SR91 temperature controller with ±0.1 °C sensitivity by using a K-type sheathed thermocouple.

The reaction section consists of a main oven (100 cm x 30 cm x 60 cm) and three vertical cylindrical reactor ovens (25 cm x 20 cm OD x 4 cm ID) inside the main oven. As abovementioned, only one of these ovens with a fixed bed 1/16'' SS tubing microreactor (37 cm x 4.5 mm ID) is used. The catalyst bed is fixed at the center of the microreactor using silane treated glass wool, and a constant-temperature zone at the center is provided via a Shimaden FP23 temperature controller with ±0.1 °C sensitivity by using a K-type sheathed thermocouple placed inside the oven. The thermocouple is placed and fixed upon an L-shaped 1/8" SS tubing and this L-shaped tubing is attached to the oven in such a way that end of the thermocouple points the center of the microreactor. This configuration is shown in Figure 3.3. Top and bottom parts of the oven are insulated by ceramic glass wool to minimize heat loss and also a fan is placed inside the main oven to have a better distribution of temperature along the main oven. The temperature of main oven is kept at 140 °C via a Shimaden SR91 temperature controller with ±0.1 °C sensitivity by using a K-type sheathed thermocouple.

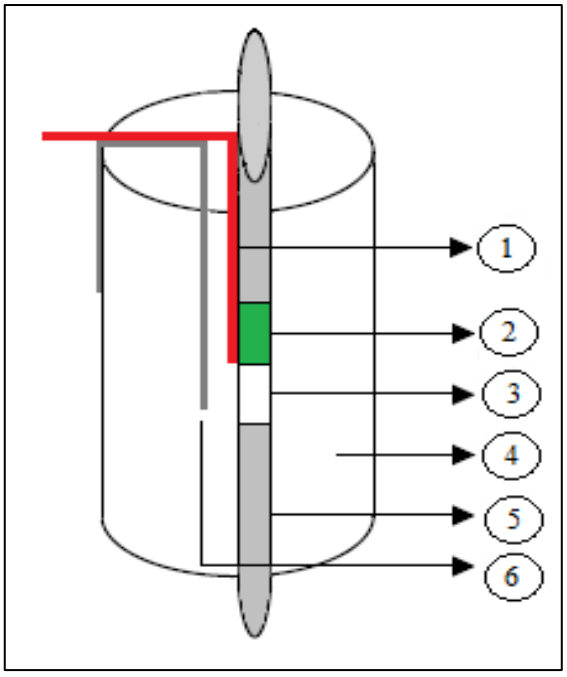

Figure 3.3. Schematic diagram of the reactor and oven system:
1. Thermocouple, 2. Catalyst, 3. Catalyst bed, 4. Oven, 5. 1/4" reactor, 6. 1/8" stainless steel tubing (Başar, 2016).

The analysis section is composed of a Hiden Analytical HPR-20 Quartz Inert Capillary Mass Spectrometer equipped with a Faraday/SEM detector and 8-way manifold/diverter system connected to a computer employing MASsoft software. This instrument allows on-line and real time analysis of inlet and outlet gaseous streams. Moreover, to prevent the MS instrument from liquid water, cold traps are placed before and after first reactor and after second/third reactors. Each cold trap has two serially connected stainless steel cylinders and one coiled tubing. The FPP system enables individual OSR and any configuration of or serial OSR, WGS, and PROX operations; but only individual OSR is studied in this thesis workload.

3.3. Catalysis Preparation and Pretreatment

In this study, 0.2wt.%Pt-10wt.%Ni/δ-Al_2O_3 catalyst is prepared and used since it was previously tested, studied, and found as a promisingly active and stable catalyst for OSR by members of our group (Gökaliler, 2012; Erdinç, 2014; Başar, 2016).

To prepare the support of the catalyst, γ-Al_2O_3 pellets are sieved into 354-250 μm (45-60 mesh) particle size and dried at 150 °C for 2 hours. Then, sieved and dried γ-Al_2O_3 is calcined at 900 °C for 4 hours in a muffle furnace and δ-Al_2O_3 support is obtained.

To obtain Pt-Ni/δ-Al_2O_3 catalyst, a sequential impregnation route is applied such that first Ni is impregnated on the support, and then Pt is impregnated on dried and calcined Ni/δ-Al_2O_3. For Ni impregnation, aqueous solution of required amount nickel (II) nitrate hexahydrate salt is used with ca. 1.1 ml DI water/g support according to incipient-to-wetness impregnation method. This impregnation is performed as explained in Section 3.2.1, then Ni/δ-Al_2O_3 sample is dried overnight at 120 °C and calcined at 600 °C for 4 hours. Similarly, Pt is impregnated on Ni/δ-Al_2O_3 by using aqueous solution of tetraammineplatinum (II) nitrate with ca. 1.1 ml DI water/g support as the same procedure expressed in Section 3.2.1. The resulting bimetallic catalyst is dried overnight at 120 °C and finally calcined at 500 °C for 4 hours.

In order to activate catalyst, an in-situ reduction pretreatment altering metal oxide states of the active metals to metallic states is conducted. For this purpose, a stepwise and

temperature-programmed reduction procedure is applied. After placing the catalyst in the constant temperature zone of the microreactor, 20 ml/min hydrogen flow is started to flow through the catalyst. The temperature is increased from room temperature to 150 °C at a rate of 10 °C/min. Then, temperature is kept constant at 150 °C during 30 minutes to have adsorbed water on the catalyst removed by hydrogen flow. Next step is to raise temperature from 150 °C to 300 °C at a rate of 5 °C/min, and waiting at 300 °C during 30 minutes to remove crystalline water. After this step, the catalyst is heated up to 500 °C at a rate of 2 °C/min and finally kept at 500 °C during 4 hours. After reduction, the system is allowed to cool down under hydrogen flow down to 150 °C and then helium is used to sweep the catalyst surface below 150 °C.

3.4. OSR Reaction Tests

Individual methane OSR performance test of the FPP system is conducted in this study with 0.2wt.%Pt-10wt.%Ni/δ-Al_2O_3 catalyst. Parameters investigated in this work are temperature of the reactor, composition of the OSR feed stream (i.e. steam-to-carbon, S/C, and oxygen-to-carbon, O/C, feed ratios), and weight of the catalyst used in the reactor, W_{OSR}, (or W/F ratio). The ranges of 350-450 °C for temperature, 3-5 for S/C ratio, and 0.74-1.33 for O/C ratio are determined in the light of previous studies done by our group (Gökaliler, 2012; Erdinç, 2014; Başar, 2016). For W_{OSR} parameter, the range of 150-200 mg catalyst is selected since 150 mg of catalyst was used previous studies giving less than 100% methane conversion and it is desired to increase the conversion with rising catalyst weight. Feed flow rates are arranged with a basis of 14 ml/min CH_4 and inert He is used to balance total flow rate of 100 ml/min, resulting W/F ratio of 1.50-2.00. Experimental conditions are presented in Table 3.4.

Box-Behnken design consisting of 4 factors/parameters is used to construct experimental plan since it has certain advantages over other experimental design methods such as central composite design. Generally, reduced number of experiments and not containing extreme conditions of all levels at the same time are advantages of Box-Behnken design allowing to obtain statistical models via response surface methodology. Even if a statistical model according to data found through these experiments is not generated in this

study, this experimental design scheme used provides a possibility of further statistical modelling (Ferreira *et al.*, 2007).

Table 3.4. Experimental conditions for individual methane OSR reaction tests.

Set #	W_{OSR}, mg (W/F)	T (°C)	Feed Flow rates (ml/min)				Feed Conditions	
			CH_4	O_2	H_2O	He	S/C	O/C
1	150 (1.50)	350	14	6.7	56	23.3	4	0.95
2	200 (2.00)	350	14	6.7	56	23.3	4	0.95
3	150 (1.50)	450	14	6.7	56	23.3	4	0.95
4	200 (2.00)	450	14	6.7	56	23.3	4	0.95
5	150 (1.50)	400	14	6.7	42	37.3	3	0.95
6	200 (2.00)	400	14	6.7	42	37.3	3	0.95
7	150 (1.50)	400	14	6.7	70	9.3	5	0.95
8	200 (2.00)	400	14	6.7	70	9.3	5	0.95
9	150 (1.50)	400	14	9.3	56	20.7	4	1.33
10	200 (2.00)	400	14	9.3	56	20.7	4	1.33
11	150 (1.50)	400	14	5.2	56	24.8	4	0.74
12	200 (2.00)	400	14	5.2	56	24.8	4	0.74
13	175 (1.75)	350	14	6.7	42	37.3	3	0.95
14	175 (1.75)	450	14	6.7	42	37.3	3	0.95
15	175 (1.75)	350	14	6.7	70	9.3	5	0.95
16	175 (1.75)	450	14	6.7	70	9.3	5	0.95
17	175 (1.75)	350	14	9.3	56	20.7	4	1.33
18	175 (1.75)	450	14	9.3	56	20.7	4	1.33
19	175 (1.75)	350	14	5.2	56	24.8	4	0.74
20	175 (1.75)	450	14	5.2	56	24.8	4	0.74
21	175 (1.75)	400	14	9.3	42	34.7	3	1.33
22	175 (1.75)	400	14	9.3	70	6.7	5	1.33
23	175 (1.75)	400	14	5.2	42	38.8	3	0.74
24	175 (1.75)	400	14	5.2	70	10.8	5	0.74
25	175 (1.75)	400	14	6.7	56	23.3	4	0.95

When these conditions are taken into consideration, catalyst amount of 150-200 mg and constant total inlet flow rate of 100 ml/min results in a W/F ratio of 1.50-2.00 mg.min/ml and a space velocity (GHSV) of 30,000-40,000 ml/(h.g-cat). In the reaction tests, corresponding catalyst amount is placed in the constant temperature zone of OSR microreactor and performance tests are conducted. Product analysis is performed ca. 2 hours time-on-stream (TOS) when clear steady state product compositions are observed.

4. RESULTS AND DISCUSSION

One of the most promising energy production technology providing non-intermittent, on-site electricity in distributed, small scale sites is PEMFC systems utilizing hydrogen as the fuel. Due to lack of well-established hydrogen distribution network, an on-site hydrogen production unit, called fuel processor, should be integrated to PEMFC as fuel processor-PEMFC (FP-PEMFC) system. Hydrogen can be produced from various hydrocarbons, including renewable sources like bio-methane, by using fuel processors. A typical fuel processor (FP) consists of three units: a reforming unit producing hydrogen rich effluent stream with considerable CO content; a WGS unit for enriching reformate with additional hydrogen while decreasing CO content, and a PROX unit to clean up CO, since CO concentrations higher than 100 ppm is practically poisonous for PEMFC. There are three reaction options for a reforming unit of an FP: steam reforming (SR), partial oxidation (POX) and oxidative steam reforming (OSR), which is the combination of SR and TOX enabling high hydrogen production activity at lower temperatures owing to heat generated by TOX on the catalyst surface providing energy to the active sites catalyzing simultaneous, highly endothermic SR. As OSR is the mostly preferred option for the reforming unit of a small scale FP, and methane is the hydrocarbon feed which has well established distribution network; optimization of the operating conditions of methane OSR reactor is of a crucial importance not only for the performance of FP but also for the overall performance of FP-PEMFC system.

The aim of this study is to determine the optimum operating parameters of the methane OSR unit of the Fuel Processor Prototype-FPP yielding high methane conversion activity with suppressed H_2/CO product selectivity. In this context, the performance of the OSR catalyst was determined and analyzed through an experimental study using temperature, S/C and O/C ratios of the feed, and the catalyst weight (or residence time, W/F) as the experimental parameters whose levels were determined by Box-Behnken experimental design. Additionally, a thermodynamic analysis was also performed for the same operation conditions in order to form a comparison basis for evaluating the performance test results, and for better understanding of the nature of OSR as well. The results are presented and discussed in two sections which are steady state performance analysis of methane OSR over

Pt-Ni/δ-Al_2O_3 catalyst and comparative analysis of performance test results with the results of the thermodynamic calculations.

4.1. Steady State Performance Analysis of Methane OSR over Pt-Ni/δ-Al_2O_3 Catalyst

Certain methane and propane OSR performance tests and kinetic studies over Pt-Ni/δ-Al_2O_3 catalysts had been performed previously by our group members (Gökaliler, 2012; Erdinç, 2014; Başar, 2016). The main motivation of this current study is to analyze the effect of operating conditions, temperature, S/C and O/C ratios of the feed, and especially the effect of catalyst weight change, *in other words the change in W/F for the same flow condition,* on the OSR performance of Pt-Ni/δ-Al_2O_3. Performance tests were conducted for the conditions given in Table 3.4 with a constant total inlet flow rate of 100 ml/min for each experiment. Methane conversion percentage was calculated according to Equation 4.1, where molar flow rates (F) were found from volumetric flow rates via using the ideal gas law. Since the stoichiometry of methane OSR, involving more than one reaction, is not 1:1; concentration and volumetric flow rate of inert in the inlet and outlet stream was used as the basis to calculate volumetric flow rates of the product gasses. The inlet and outlet concentrations were measured by MS connected to the FPP system.

$$CH_4\ Conversion\ (\%) = \frac{F_{CH_4,in} - F_{CH_4,out}}{F_{CH_4,in}} \tag{4.1}$$

OSR is an intricate overall reaction as it consists of a group of chemical reactions having completely different thermodynamic properties, energetics, speed and kinetics; those reactions include steam reforming reactions, partial and total oxidation reactions, undesired methanation reactions and even WGS reaction. Due to this complexity of methane OSR, interpreting and discussing the results obtained through the current experimental study (i.e. CH_4 conversions and product concentrations) are rather a difficult task, especially when it comes to the changes in performance specs in response to the changes in W/F (see Sections 4.1.4 and 4.2.2 for a detailed analysis). The results of steady state methane OSR performance tests are presented and discussed in four sections, in which the effects of temperature, S/C feed ratio, O/C feed ratio and W/F on catalyst performance are scrutinized respectively. It

should be noted that, as in all experiments O_2 fed top the reactor is completely consumed, O_2 concentration is not explicitly reported anywhere in the following sections.

The construction of a Box-Behnken experimental design leads to comparisons in such a way that the effect of each parameter on performance is examined for maximum and minimum levels of one other parameters, and at intermediate levels of rest of the parameters at each stage; e.g. effect of temperature is examined at high and low levels of W/F and intermediate levels of S/C ratio and O/C ratio, then at high and low levels of S/C ratio and intermediate levels of O/C ratio and W/F , and so forth. This reasoning will be discussed in Sections 4.1.1, 4.1.2, 4.1.3 and 4.1.4 in a more detailed fashion.

4.1.1. The Effect of Temperature on Methane OSR

CH_4 conversion percentages and steady state performance results of the OSR with respect to temperature at different conditions are presented in Table 4.1 and Figure 4.1, respectively. As the tests were conducted according to Box-Behnken experimental design, the effect of each parameter is examined at the extremes of every parameter, while the other parameters are kept constant at their intermediate values.

Temperature rise caused a significant increase of CH_4 conversion for all conditions as can be seen in Table 4.1, without any exception. This can be explained by the fact that as the temperature increase yields higher reaction specific rate constants and thus higher rates for all reactions, and many of those involved in OSR are methane-consuming reactions; CH_4 conversion percentage considerably rose with increasing temperature. Additionally, with the assumption that oxidation reactions (TOX and POX) are irreversible, temperature rise favored endothermic CO and CO_2-forming steam reforming reactions over exothermic back methanation of CO and CO_2.

Table 4.1. CH_4 conversion percentages with respect to temperature.

Couple	Set #	W/F (mg.min/ml)	S/C	O/C	T (ºC)	CH_4 Conversion (%)
(a)	1	1.50	4	0.95	350	44.5
	3		4	0.95	450	81.8
(b)	2	2.00	4	0.95	350	37.2
	4		4	0.95	450	62.8
(c)	13	1.75	3	0.95	350	46.6
	14	1.75		0.95	450	76.3
(d)	15	1.75	5	0.95	350	41.2
	16	1.75		0.95	450	77.0
(e)	17	1.75	4	1.33	350	60.9
	18	1.75	4		450	93.5
(f)	19	1.75	4	0.74	350	34.4
	20	1.75	4		450	84.4

In addition to CH_4 conversions, dry-basis and inert-free gas concentrations of the OSR product stream varied with the OSR feed composition and reactor temperature, as presented in Figure 4.1. H_2 concentration in the product stream rose with increasing temperature, and this rise was strongly related with the increase of CH_4 conversion as most of methane-consuming reactions in OSR produce H_2. Hence, an increase in H_2 percentage in the product at higher OSR temperatures was expected and reasonable. On the other hand, CO_2 percentage in the product stream decreased with increasing temperature whereas CO percentage rose at higher temperatures. This might be caused as a result of higher endothermicity of CO producing SR compared to that of CO_2 producing SR, and, in addition, relatively higher inhibiting effect of temperature rise on TOX, which is much more exothermic compared to POX. In an overall evaluation, higher temperatures promoted CO-producing SR more than CO_2-producing SR, while -partially- suppress CO_2 producing TOX more than CO producing POX. In all cases shown in Figure 4.1, rising temperature reduced H_2/CO product ratio. That basically stemmed from relatively higher increase in CO in the product compared to that of the rise in H_2. Furthermore, as it is slightly endothermic and

favored at high temperatures, reverse WGS (RWGS) might also be partially responsible for the drop in H_2/CO product ratio; as the catalyst used showed equilibrium-limited HTS activity at lower OSR temperatures, the escalated H_2 concentration at high temperatures favored its RWGS activity consuming H_2 while producing CO.

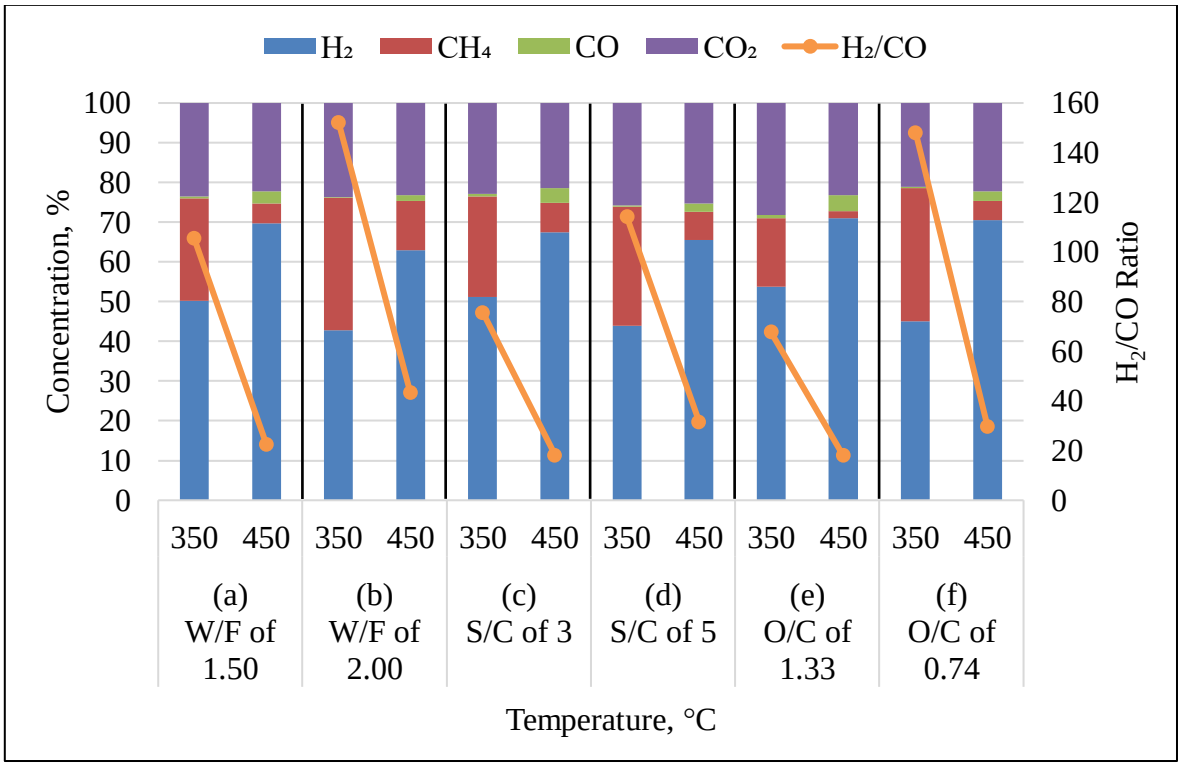

Figure 4.1. Steady state performance results comparison with temperature at different conditions (Set 1-3, Set 2-4, Set 13-14, Set 15-16, Set 17-18, Set 19-20, respectively).

4.1.2. The Effect of Steam-to-Carbon Ratio on Methane OSR

The change in catalyst activity, in terms of CH_4 conversion, in response to change in S/C feed ratio at for the conditions determined by Box-Behnken design are presented in Table 4.2. Except for one parameter combination at 350 °C, CH_4 conversion increased, either slightly or significantly, in response to rising temperature. Since steam, H_2O, is a reactant of both CO and CO_2-producing SR reactions, and a product of CO producing back methanation and CO_2 producing methanation reactions; in an overall evaluation, rise in CH_4 conversion

at higher S/C ratio indicated that both SR reactions were favored whereas both methanation reactions were inhibited for given conditions. On the contrary, at 350 °C, low temperature brought highly exothermic methanation reactions into prominence leading to a decrease in measured CH_4 conversion when the feed became rich in steam with the increase in S/C ratio. From another point of view, higher H_2O concentration might limit TOX reaction which supplies required heat for SR reactions, and thus highly endothermic SR reactions suffered from the lack of heat.

Table 4.2. CH_4 conversion percentages with respect to S/C ratio.

Couple	**Set #**	**W/F (mg.min/ml)**	**T (ºC)**	**O/C**	**S/C**	**CH_4 Conversion (%)**
(a)	5	1.50	400	0.95	3	45.9
	7		400	0.95	5	65.6
(b)	6	2.00	400	0.95	3	46.1
	8		400	0.95	5	75.7
(c)	13	1.75	350	0.95	3	46.6
	15	1.75		0.95	5	41.2
(d)	14	1.75	450	0.95	3	76.3
	16	1.75		0.95	5	77.0
(e)	21	1.75	400	1.33	3	52.4
	22	1.75	400		5	63.9
(f)	23	1.75	400	0.74	3	46.5
	24	1.75	400		5	48.6

The changes observed in dry-based and inert-free steady state gas concentrations in OSR product stream in response to the changes in S/C feed ratio are presented in Figure 4.2. The couples (a) and (b), which were conducted over 150 and 200 mg catalyst, demonstrated an expected trend; increasing H_2, CO and CO_2 concentrations with rising S/C ratio can be explained through the favored SR by increased steam in the feed leading higher production of H_2, CO and CO_2. As incremental CO rise was higher than that of H_2 rise in response to

the increase in S/C ratio, H_2/CO product ratio decreased. On the other hand, the couples (c) and (d), shown by 350 and 450 °C on x-axis, the situation was complicated. The result hinted that CO_2 producing SR and/or TOX were/was more favored compared to that of CO producing SR and/or POX, and CO methanation became relatively dominant. Even though H_2 concentration decreased with increasing S/C ratio, the proportionally greater decline in CO concentration led to decrease in H_2/CO product ratio. The trends obtained in the couples (e) and (f) shown in Figure 4.2 were very similar to that of the couples (a) and (b) indicating a rise in S/C feed ratio favoring SR reactions. On the other hand, for the couples (e) and (f), the incremental rise in H_2 concentration was higher compared to that of CO rise, therefore H_2/CO ratio increased slightly for the couple (e) and significantly for the couple (f), respectively.

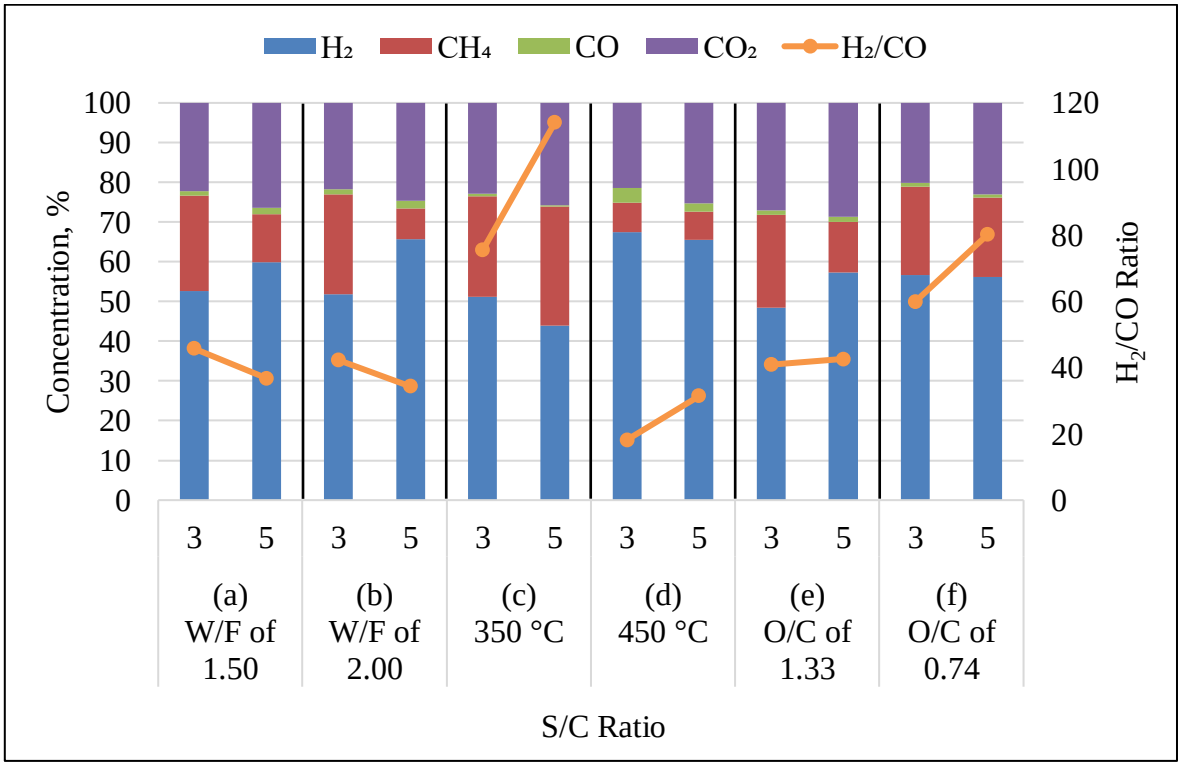

Figure 4.2. Steady state performance results comparison with S/C ratio at different conditions (Set 5-7, Set 6-8, Set 13-15, Set 14-16, Set 21-22, Set 23-24, respectively).

4.1.3. The Effect of Oxygen-to-Carbon Ratio on Methane OSR

The change in CH_4 conversion in response to change in O/C feed ratio is presented in Table 4.3. An increase in O/C ratio caused a definite rise in CH_4 conversion for all conditions, which was led by strong increase in POX and TOX. Since O_2 is a reactant for only POX and TOX reactions and it is not directly related to SR, methanation, and WGS reaction; an increase in O/C ratio straightly boosted CH_4 conversion through favoring POX and TOX. On the other hand, the rise in O/C feed ratio affected SR reactions indirectly through favoring SR via increasing heat produced by oxidation reactions, while impeding SR through decreasing the amount of methane available.

Table 4.3. CH_4 conversion percentages with respect to O/C ratio.

Couple	**Set #**	**W/F (mg.min/ml)**	**T (ºC)**	**S/C**	**O/C**	**CH_4 Conversion (%)**
(a)	11	1.50	400	4	0.74	54.6
	9		400	4	1.33	66.1
(b)	12	2.00	400	4	0.74	43.6
	10		400	4	1.33	56.3
(c)	19	1.75	350	4	0.74	34.4
	17	1.75		4	1.33	60.9
(d)	20	1.75	450	4	0.74	84.4
	18	1.75		4	1.33	93.5
(e)	23	1.75	400	3	0.74	46.5
	21	1.75	400		1.33	52.4
(f)	24	1.75	400	5	0.74	48.6
	22	1.75	400		1.33	63.9

Figure 4.3 demonstrates the change in dry-basis and inert-free steady state gas concentrations in the OSR product streams in response to the change in O/C feed ratio. The increased O/C feed ratio resulted in a significant increase in CO and CO_2 concentrations via

favoring POX and TOX, whereas it decreased CH_4 concentration limiting hydrogen production. Resultantly, lowered H_2 and increased CO concentrations in the product in response to increase in O/C feed ratio resulted in lowered H_2/CO product ratio for all experimental couples.

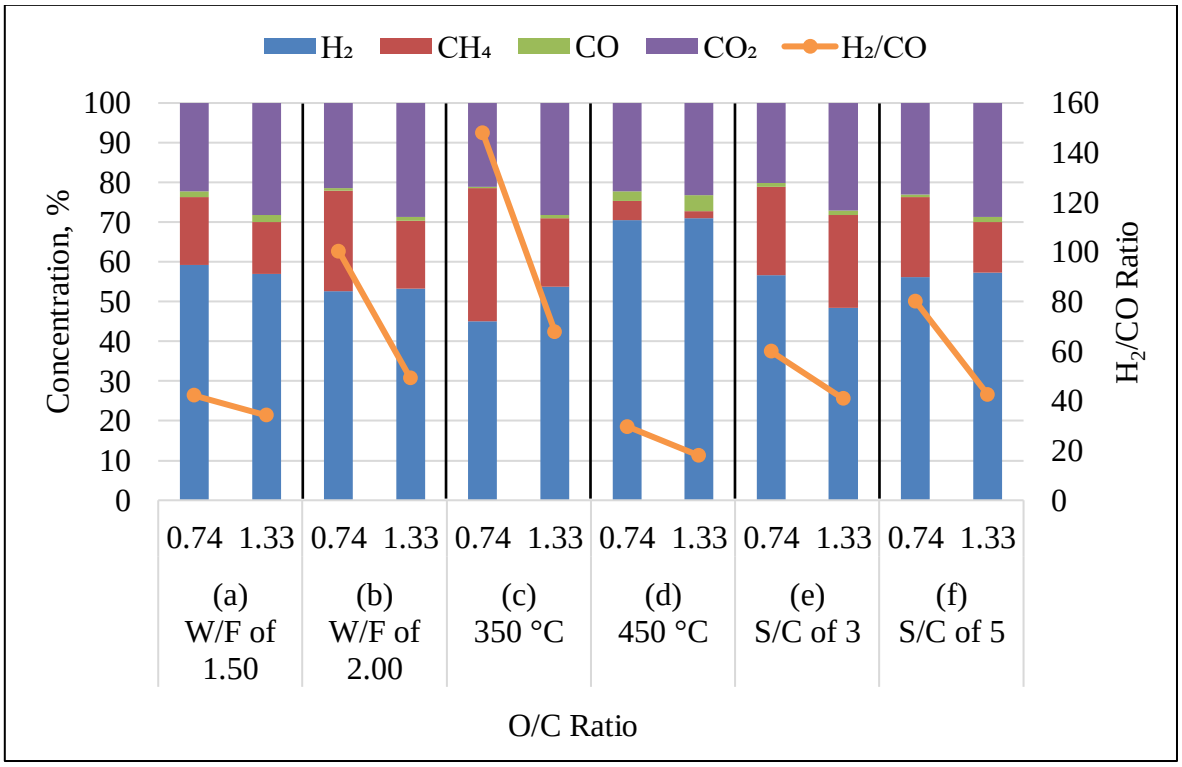

Figure 4.3. Steady state performance results comparison with O/C ratio at different conditions (Set 11-9, Set 12-10, Set 19-17, Set 20-18, Set 23-21, Set 24-22, respectively).

4.1.4. The Effect of W/F on Methane OSR

The change in CH_4 conversion levels in response to W/F (or catalyst weight) are presented in Tables 4.4 and 4.5. Table 4.4 presents expected, at least acceptable, trends of conversion-W/F relations. For a single chemical reaction, reactants are converted to products along the catalyst bed and conversion increases with the amount of catalyst till equilibrium limitation even if the reaction is reversible. The experimental couple (d) at S/C ratio of 5 (Set # 7&8) was very traditional in terms of this relation; there was a significant increase in the conversion with the increase in W/F. However, for the couple (c) with S/C ratio of 3 (Set

5&6) the conversion increase was very limited though the increase in W/F is ca. 35%; this result hinted the intricate nature of OSR reaction having a very complex mechanism.

Table 4.4. Increasing CH_4 conversion percentages with increased W/F.

Couple	**Set #**	**T (°C)**	**S/C**	**O/C**	**W/F (mg.min/ml)**	**CH_4 Conversion (%)**
(c)	5	400	3	0.95	1.50	45.9
	6	400		0.95	2.00	46.1
(d)	7	400	5	0.95	1.50	65.6
	8	400		0.95	2.00	75.7

The results of the other performance tests at different conditions showed remarkable decreases in CH_4 conversion level in response to a rise in W/F, as shown in Table 4.5. That was mainly caused by the existence of many reactions, simultaneous or in series, constituting OSR. It is also noteworthy that that reactions constituting OSR even take place at different regions along the catalyst bed owing to their distinct differences in terms of thermodynamics and kinetics. Immediate POX and TOX reactions are dominant at the entrance region of the catalyst bed, while slower and endothermic SR reactions dominantly occur just following these exothermic oxidation reactions owing to the help of heat generated by POX and TOX reactions as SR reactions require much higher temperatures on the catalyst surface to proceed, i.e. far greater than the reactor temperature, 450 °C, unless oxidation reactions exist. Moreover, the decrease in CH_4 conversion with increasing W/F indicated that methanation reactions take place even following SR reactions, as long as the bed length is enough, as there is no any other reaction that produces methane decreasing apparent methane conversion. The fall in CH_4 conversion level indicated in Table 4.5 in response to increase in W/F was due to back methanation reactions occurring in region close to the exit of the bed following SR reactions. The trends observed strongly suggested the necessity of scrutinizing the relation between space time/space velocity and reactor performance (i.e. methane conversion, H_2 production, H_2/CO selectivity) in order to reach optimal reaction conditions for OSR reactor.

Table 4.5. Decreasing CH_4 conversion percentages with increased W/F.

Couple	**Set #**	**T (ºC)**	**S/C**	**O/C**	**W/F (mg.min/ml)**	**CH_4 Conversion (%)**
(a)	1	350	4	0.95	1.50	44.5
	2		4	0.95	2.00	37.2
(b)	3	450	4	0.95	1.50	81.8
	4		4	0.95	2.00	62.8
(e)	9	400	4	1.33	1.50	66.1
	10	400	4		2.00	56.3
(f)	11	400	4	0.74	1.50	54.6
	12	400	4		2.00	43.6

Figure 4.4 presents comparative analysis of dry-based and inert-free steady state gas concentrations in the OSR product stream and W/F that the reaction conducted over. Except the couples (c) and (d), which were the experiments at S/C ratio of 3 and 5, having different behavior in terms of CH_4 conversion change in response to W/F increase; for those, H_2 concentrations were reduced in an agreement with the decline in CH_4 conversion for higher W/F. When the increase in H_2/CO product ratio were considered, relative decrease in CO concentration in product were greater than that of H_2 leading hinting favoring of CO-consuming methanation reaction with further rise in W/F. CO_2 concentration stayed nearly the same unaffected by increase in W/F for the couples (a) and (e), whereas small increase was observed for the couple (b), which had a substantial decrease in CO concentration. On the other hand, CO_2 concentration in couple (f) was decreased with the rise in W/F, which implied CO_2 methanation was also favored in response to increase in W/F.

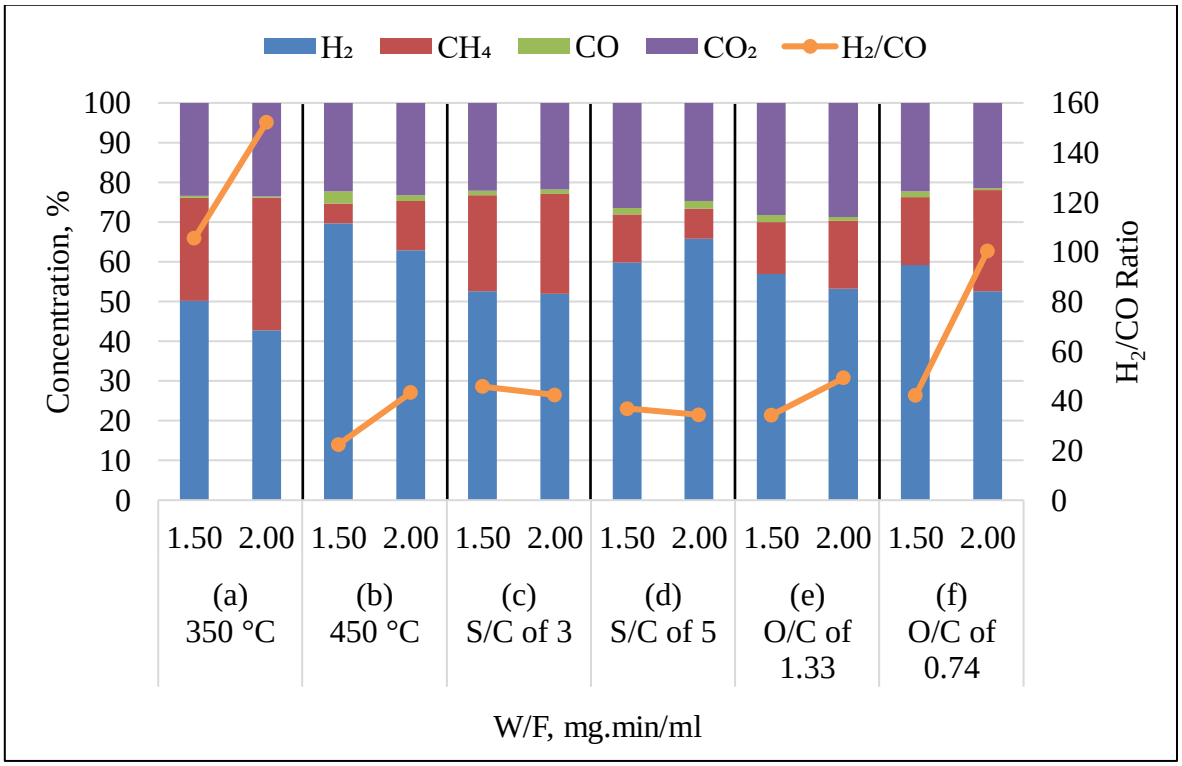

Figure 4.4. Steady state performance results comparison with W/F at different conditions (Set 1-2, Set 3-4, Set 5-6, Set 7-8, Set 9-10, Set 11-12, respectively).

When the other couples were considered, the results obtained for S/C of 3 in Figure 4.4, the couple (c), showed very insignificant changes in concentrations of gases in OSR product stream with the rise in W/F. On the contrary, H_2 concentration of the couple (d) in Figure 4.4 rose significantly with decreases in CO_2 and CH_4 concentrations, which reflected that CO_2 consuming SR reaction was favored with the increase in W/F. The fall in H_2/CO ratio indicated that proportional CO concentration increase was higher than that of H_2.

4.2. Thermodynamic Comparison Analysis of the Experimental Results

Thermodynamic CH_4 conversion were calculated by using HSC Chemistry 5.11 software utilizing the minimization of Gibbs free energy of the given system. There are similar studies in the literature which had used HSC Chemistry program for thermodynamic

analysis (Sato *et al.*, 2010; Wang *et al.*, 2010; Zeng *et al*., 2010; Wang *et al*., 2011; Wang *et al.*, 2012). The program requires both reactant and product chemical species in the system along with the inlet feed composition. In the current work, by considering all reactions run during OSR, as listed in Chapter 2, and for the given feed compositions; thermodynamic product compositions were obtained for a given temperature interval by HSC.

It should be noted that HSC software utilizes species instead of reactions, and consequently, it implicitly includes WGS and PROX reactions in addition to SR and TOX in the evaluation of OSR. Even though WGS and PROX reactions can be seen as irrelevant, these reactions are both included in discussing the results of the experimental studies as it has been known that Pt-Ni/δ-Al_2O_3 catalyst shows especially pronounced WGS activity. On the other hand, as CH_4 is a reactant and a product in only OSR reaction, Section 4.2.1 is devoted only to the comparative analysis of CH_4 conversion trends observed in performance tests and calculated through thermodynamics in response to changes in temperature, and S/C and O/C feed ratios; while a complete analysis of the trends in CH_4 conversion, H_2 product concentration, and H_2/CO product ratio as a function of W/F are discussed in Section 4.2.2, where experimental results obtained for different W/F values are comparatively analyzed with the thermodynamic calculation results, corresponding practically W/F value of infinity, in order to both elucidate the effect of W/F in catalyst performance and to guess the possible W/F value region that may lead optimum performance.

4.2.1. Thermodynamic Consistency Analysis: Effects of Temperature, and S/C and O/C Feed Ratios on Methane Conversion

Thermodynamic CH_4 conversion values for the temperature interval used in performance tests, 350-450 °C, for the experimentally used S/C and O/C feed ratio values are presented in Figures 4.5 and 4.6, respectively. The parametric effect of W/F on CH_4 conversion, hydrogen content of the product and H_2/CO ratio of the product stream will be compared and discussed in Section 4.2.2.

The results show that for all inlet conditions, the increase in temperature results in a significant increase in thermodynamic CH_4 conversion (Figure 4.5 and 4.6). Thus, thermodynamic calculation results confirmed the validity of reasoning presented in 4.1.1 on the effect temperature increase on experimental CH_4 conversion. When OSR reactions were considered, POX and TOX reactions were practically assumed irreversible, and highly endothermic SR reactions were favored with the increase in temperature. Significant increase in thermodynamic CH_4 conversion with the increase in temperatures support the idea that overall OSR is endothermic, and thus SR is most probably the dominating reaction for the given conditions.

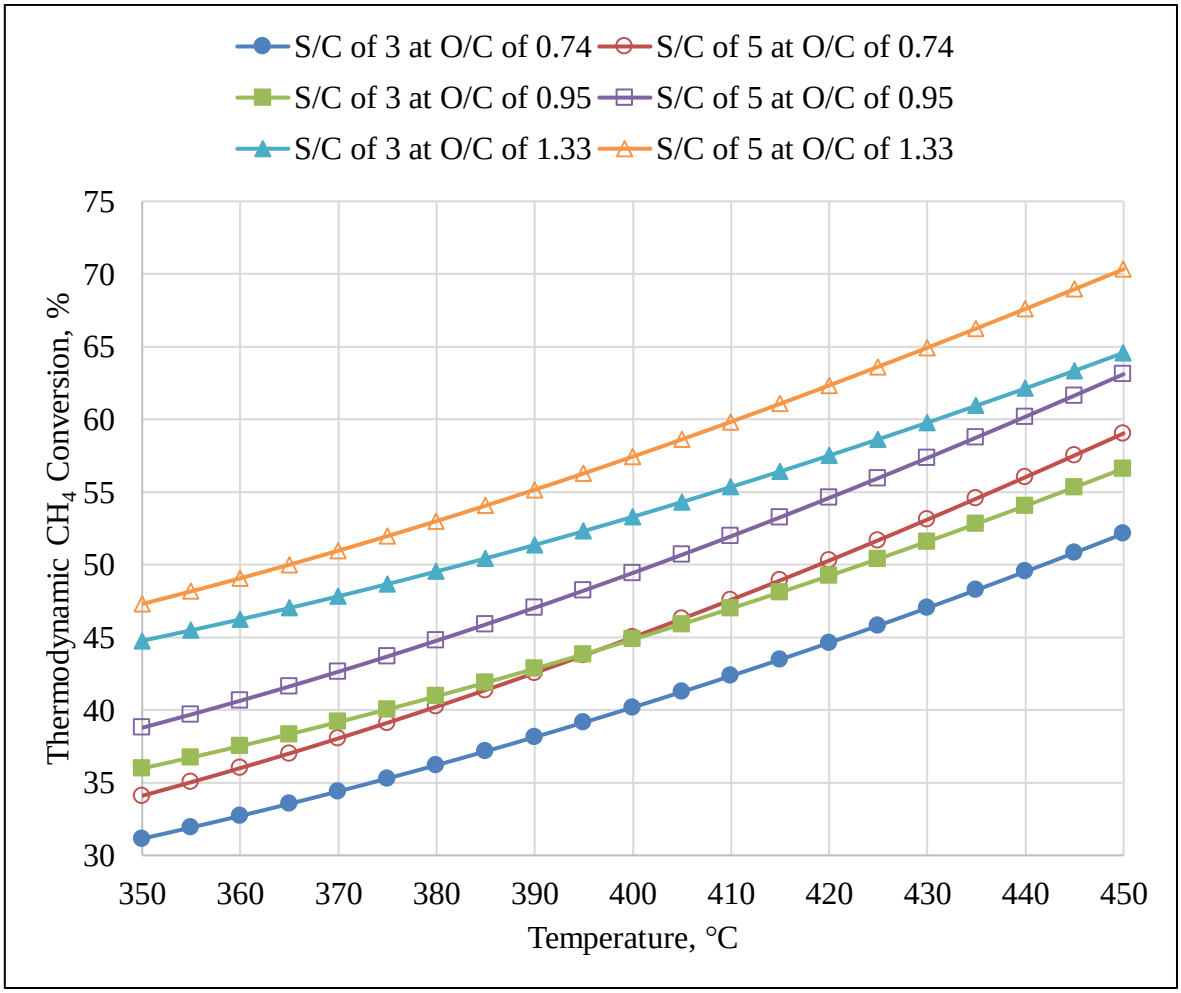

Figure 4.5. Thermodynamic CH_4 conversion percentages comparison with changing S/C ratios at different O/C ratios (feed conditions of Set 23, Set 24, Set 5-6, Set 7-8, Set 21, and Set 22, respectively).

Figure 4.5 demonstrates the effect of S/C on thermodynamic CH_4 conversion limit for different O/C feed ratio levels for 350-450 °C temperature interval. For all O/C feed ratios, thermodynamic CH_4 conversion increases in response to rise in S/C ratio for the whole temperature interval. The trends in experimental results are in accordance with the thermodynamic trends presented in Figure 4.5. The rises in thermodynamic CH_4 conversion with the increase in S/C ratio can be explained by favored SR reactions, which is the same reasoning mentioned in discussing the experimental results in Section 4.1.2.

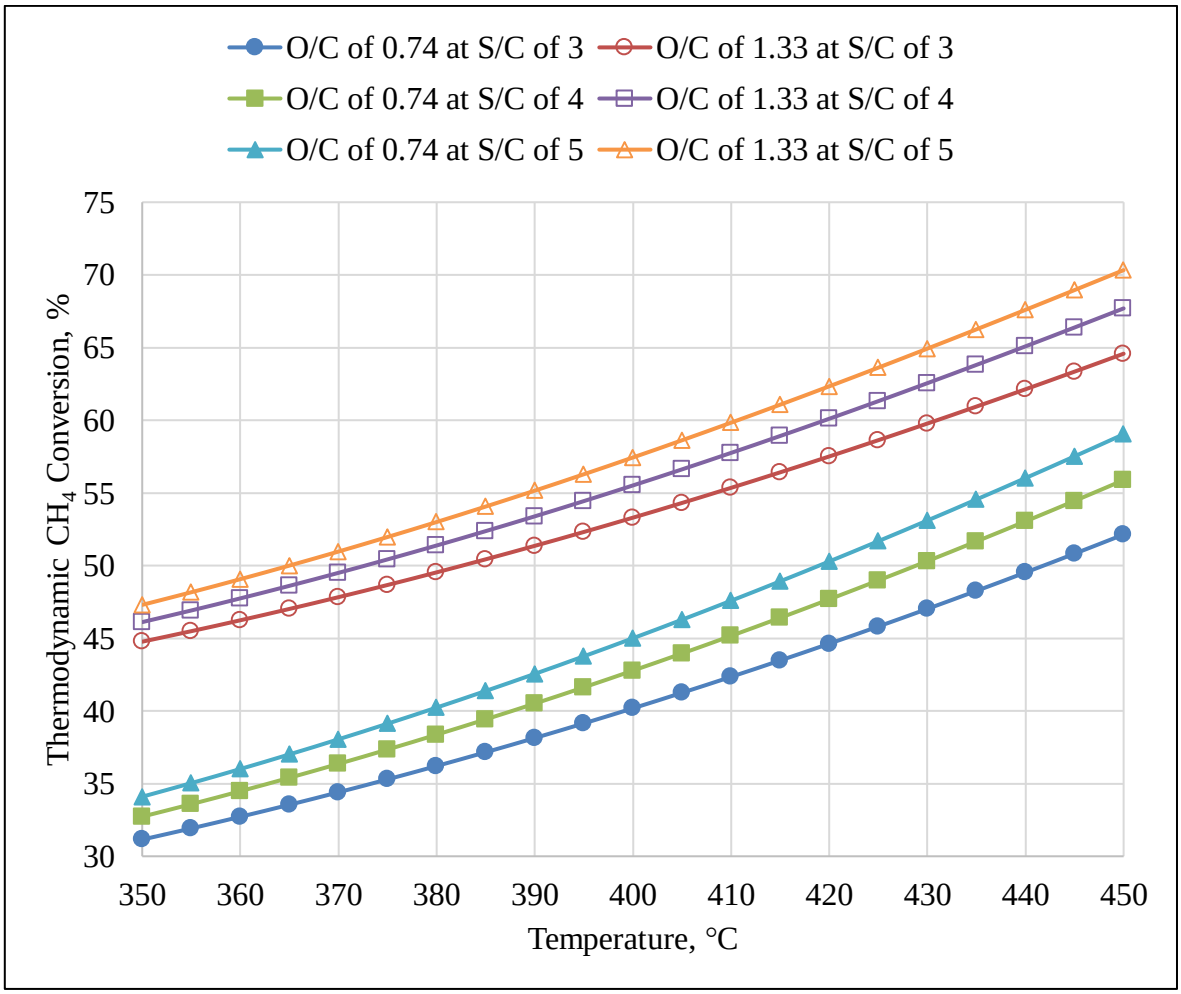

Figure 4.6. Thermodynamic CH_4 conversion percentages comparison with changing O/C ratios at different S/C ratios (feed conditions of Set 23, Set 21, Set 11-12, Set 9-10, Set 24, and Set 22, respectively).

The effect of O/C on thermodynamic CH_4 conversion limit for different S/C feed ratio levels for 350-450 °C temperature interval is presented in Figure 4.6. For all S/C feed ratio values, thermodynamic CH_4 conversion shows a significant increase in response to an increase in O/C ratio for the whole temperature interval. In fact, the relative increase in thermodynamic CH_4 conversion as a function of rise in O/C ratio is much greater compared to the one observed in response to a rise in S/C ratio. Even though O/C feed ratio does not directly favor SR reaction, in contrast with the case for S/C ratio, the increase in heat generated by POX and TOX reactions due to increased O/C ratio most probably more effective than an increment of S/C ratio in terms of favoring SR reaction. It can be inferred that OSR is more sensitive to level of heat production compared to that of the steam and methane concentrations for the reaction conditions studied. Thermodynamic results showing significant increase in CH_4 conversion with an increase in O/C feed ratio are in agreement with the trends observed in experimental findings.

4.2.2. Combined Experimental and Thermodynamic Evaluation of the Relation between CH_4 Conversion and W/F

Thermodynamic conversion level is considered as the upper conversion limit for a reaction that can be reached for the specified feed conditions at the given temperature. Thermodynamic conversion and product distribution implicitly calculated for the case the reactants spend infinite time in a reactor; there the presence or absence of a catalyst has no effect on neither conversion nor product distribution. Thus, if for a hypothetical single elementary reaction, once the average time spend inside the reactor exceeds the time necessary to reach thermodynamic conversion, no further change occurs in conversion and product distribution. On the other hand, OSR is an intricate reaction system involving many elementary reactions, having completely different energetics and speeds, proceed both in serial and parallel fashion. Additionally, if H_2, which is the valuable product, builds up anywhere in the reactor, it may be further react to give unwanted methane and/or water; thus, when W/F is not optimized, the reactor effluent has H_2 concentration far lower than its maximum inside the reactor whilst still higher than that at thermodynamic limit. The situation is just the opposite for methane; back methanation may lead experimental

conversion higher than the corresponding thermodynamic conversion level. Figure 4.7 demonstrates experimental CH_4 conversions observed for W/F of 1.50 and 2.00 mg.min/ml, and thermodynamic CH_4 conversion for the corresponding cases at the W/F of infinity (∞).

In accordance with the possibility of back methanation, experimental CH_4 conversion percentages reached for W/F ratios of 1.50 and/or 2.00 mg.min/ml were higher than thermodynamic CH_4 conversion percentages for all cases shown in Figure 4.7. These results clearly indicated that methanation reactions producing CH_4 became favored following both due to SR reaction, decreasing CH_4 concentration in the stream, and increased H_2 due to both SR and HTS. The results show that for longer catalyst bed, CH_4 conversion should approach to a lower value than the observed experimental conversions for the given experimental conditions. This situation is evident even for W/F rise from 1.50 to 2.00 for the couples (a), (b), (e), and (f) in Figure 4.7.

The analysis clearly show that further W/F increase, above 2.00, does not enhance catalytic performance in terms of CH_4 conversion. Besides, thermodynamic CH_4 conversion levels revealed that further rise in W/F was not desired to maximize CH_4 conversion for any of these cases, even for the couples (c) and (d) having an increase in CH_4 conversion percentage with an experimental raise in W/F. Actually, there should be different optimum W/F ratios resulting in maximum CH_4 conversion levels for each case studied, e.g. optimum W/F yielding maximum CH_4 conversion for the couples (c) and (d) is greater than 1.50 mg mg.min/ml whereas optimum W/F ratios yielding maximum CH_4 conversion for the couples (a), (b), (e), and (f) were less than 2.00 mg.min/ml, and maybe even less than 1.50 mg.min/ml.

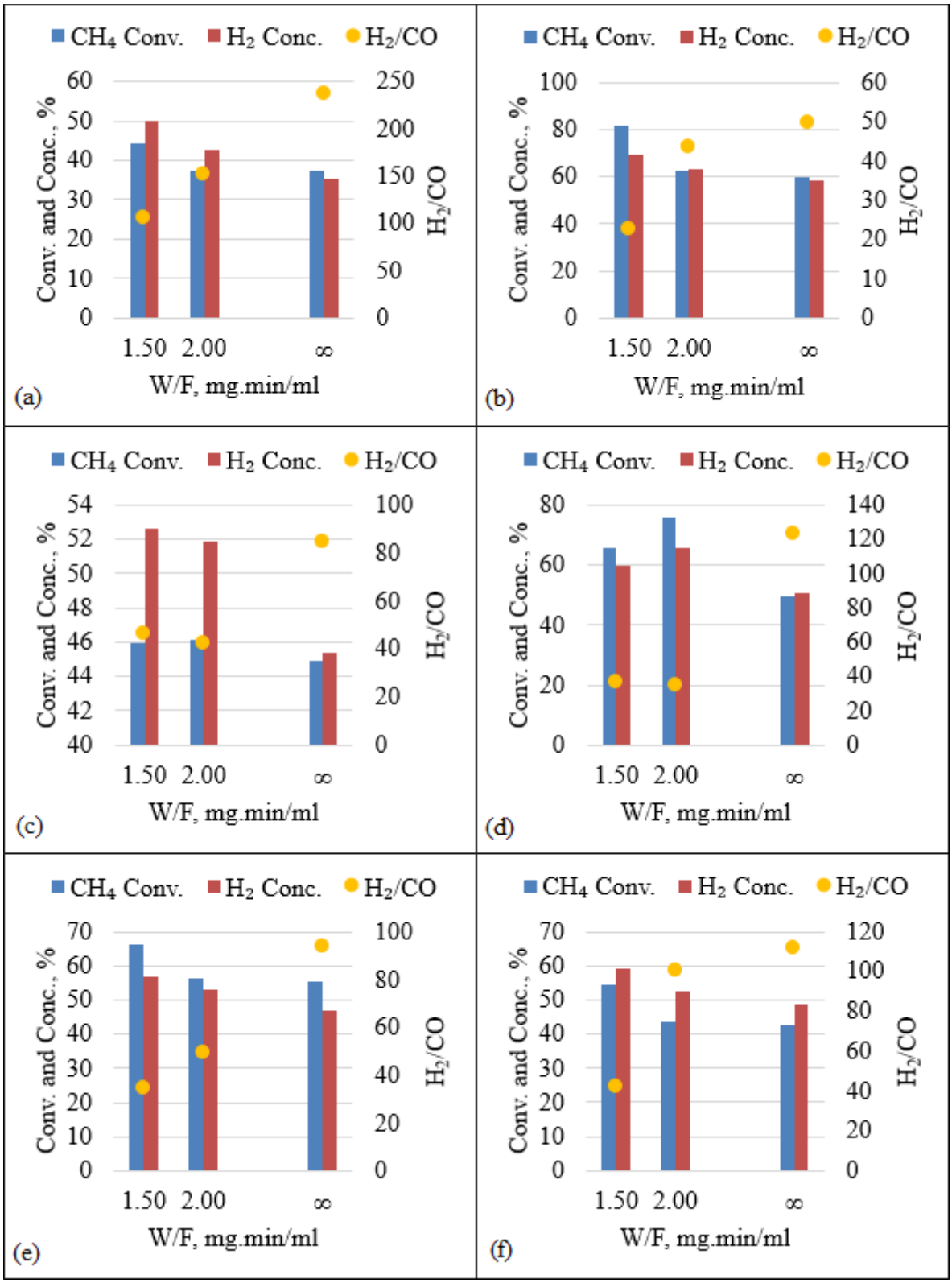

Figure 4.7. Experimental and thermodynamic CH_4 conversion and H_2 concentration percentages, and H_2/CO ratio with respect to W/F

(a) Set 1-2 (b) Set 3-4 (c) Set 5-6 (d) Set 7-8 (e) Set 9-10 (f) Set 11-12.

All couples presented in Figure 4.7 had a lower thermodynamic dry-basis inert-free H_2 product concentration and a higher thermodynamic H_2/CO ratio compared to experimental cases. A comparative analysis indicates that extent of decrease in CO concentration is higher than that of H_2 yielding higher H_2/CO ratio with the increase in W/F, and the maximum H_2/CO ratio calculated for thermodynamic equilibrium. Consequently, when one tries to find the optimum conditions yielding both highest possible H_2 concentration and highest H_2/CO ratio at the same time, he/she should deal with a Pareto optimal for W/F value as H_2 and H_2/CO trends as a function of W/F are -in general- opposite. Another complication comes from the fact that the degree of decrease and increase in H_2 concentration and H_2/CO ratio, respectively, in response to rise in W/F strongly depends on S/C and C/O of the feed, at least up to some practical W/F levels. This most probably stems from the fact that above mentioned trends are directly related with extent of back methanation, HTS/r-HTS and oxidation reaction.

5. CONCLUSIONS

5.1. Conclusions

The object of the current study is to determine the optimum operating parameters of the methane OSR unit of the Fuel Processor Prototype-FPP yielding high methane conversion activity with suppressed H_2/CO product selectivity over Pt-Ni/δ-Al_2O_3 catalyst, which has been designed and opted by our group, via an experimental study using temperature, S/C and O/C ratios of the feed, and the catalyst weight (or residence time, W/F) as the experimental parameters whose levels were determined by Box-Behnken experimental design. Furthermore, a thermodynamic analysis was also performed for the same operation conditions in order to establish a comparison basis for evaluating the performance test results, and for a better comprehension of the nature of OSR as well.

First, steady state performance analysis of methane OSR over Pt-Ni/δ-Al_2O_3 catalyst was experimentally studied through the experimental parameters of temperature, S/C and O/C feed ratios, and W/F ratio. Major outcomes deduced from the experimental work can be given as follows:

- When the temperature of OSR was increased, in the range of 350-450 °C, CH_4 conversion significantly increased whereas H_2 concentration and H_2/CO ratio in the product decreased.

- When S/C feed ratio of OSR was increased, in the range of 3-5, CH_4 conversion increased, excluding one exceptional case, with varying H_2 concentration and H_2/CO ratio in the product.

- When O/C feed ratio of OSR was increased, in the range of 0.74-1.33, CH_4 conversion significantly increased whereas H_2/CO ratio in the product definitely decreased.

- When W/F of OSR was increased, in the range of 1.50-2.00 mg.min/ml, CH_4 conversion mostly decreased with varying H_2 concentration and H_2/CO ratio in the

product. This unordinary situation indicated that there was a different optimum W/F for OSR in each feed condition and suggested the necessity of scrutinizing the relation between space time/space velocity and reactor performance (i.e. methane conversion, H_2 production, H_2/CO selectivity) in order to reach optimal reaction conditions for OSR reactor.

Second, a thermodynamic analysis was performed to validate the effects of the parameters of temperature, S/C and O/C feed ratios of OSR on CH_4 conversion, and also to make a complete analysis of the trends in CH_4 conversion, H_2 product concentration, and H_2/CO product ratio as a function of W/F. Main conclusions drawn from the thermodynamic analysis can be given as follows:

- When each one of the parameters of temperature, S/C and O/C feed ratios was increased, thermodynamic CH_4 conversion increased significantly. Thermodynamic results confirmed the experimental effects of these parameters on CH_4 conversion.

- When thermodynamic CH_4 conversion was calculated, i.e. when W/F was infinitely increased, it was seen that thermodynamic CH_4 conversions were lower than experimental CH_4 conversions of both 1.50 and/or 2.00 mg.min/ml. That confirmed the reasoning reached by the experimental analysis; and showed that there would be a Pareto optimal for W/F value to find the optimum conditions yielding both highest possible H_2 concentration and highest H_2/CO ratio at the same time, because H_2 and H_2/CO trends as a function of W/F were -in general- opposite.

5.2. Recommendations

For future studies, following recommendations can be taken into consideration:

- A statistical model can be constructed, thanks to the suitability of experimental data formed by a Box-Behnken experimental design, to have a further interpretation of optimal experimental conditions, even beyond the ranges experimentally investigated.

- A wider range of W/F for OSR can be studied for further analysis of optimum W/F for OSR at certain conditions.

- A similar and/or more extensive analysis can be performed for a serial OSR-WGS-PROX system for better understanding of a FP as a whole.

REFERENCES

Aartun, I., H. J. Venvik, A. Holmen, P. Pfeifer, O. Görke and K. Schubert, 2005, "Temperature profiles and residence time effects during catalytic partial oxidation and oxidative steam reforming of propane in metallic microchannel reactors", *Catalysis Today*, Vol. 110, pp. 98-107.

Asharf, M. A., G. Ercolino, S. Specchia and V. Specciha, 2014, "Final step for CO syngas clean-up: Comparison between CO-PROX and CO-SMET processes", *International Journal of Hydrogen Energy*, Vol. 39, pp. 18109-18119.

Balzarotti, R., C. Italiano, L. Pino, C. Cristiani and A. Vita, 2014, "Ni/CeO_2-thin ceramic layer depositions on ceramic monoliths for syngas production by Oxy Steam Reforming of biogas", *Fuel Processing Technology*, Vol. 149, pp. 40-48.

Başar, M. S., 2016, *A Study on Co-Free Hydrogen Production and Adsorbent Design for Selective Carbon Dioxide Removal*, Ph. D. Dissertation, Boğaziçi University.

Behling, N. H., 2013, *Fuel Cells – Current Technology Challenges and Future Research Needs*, Elsevier, Great Britain.

Carrette, L., K. A. Friedrich and U. Stimming, 2001, "Fuel Cells – Fundamentals and Applications", *Fuel Cells*, Vol. 1, pp. 5-39.

Cipiti, F., L. Pino, A. Vita, M. Lagana and V. Recupero, 2013, "Experimental investigation on a methane fuel processor for polymer electrolyte fuel cells", *International Journal of Hydrogen Energy*, Vol. 38, pp. 2387-2397.

Cutillo, A., S. Specchia, M. Antonini, G. Saracco and V. Specchia, 2006, "Diesel fuel processor for PEM fuel celss: Two possible alternatives (ATR versus SR)", *Journal of Power Sources*, Vol. 154, pp. 379-385.

Çağlayan, B. S., A. K. Avcı, Z. I. Önsan and A. E. Aksoylu, 2005, "Production of Hydrogen over Bimetallic Pt-Ni/δ-Al_2O_3: I. Indirect Partial Oxidation of Propane", *Applied Catalysis*, Vol. 280, pp. 181-188.

Çağlayan, B. S. and A. E. Aksoylu, 2009, "Water-Gas Shift Reaction over Bimetallic Pt-Ni/Al_2O_3 Catalysts", *Turkish Journal of Chemistry*, Vol. 33, pp. 249-256.

Çağlayan, B. S. and A. E. Aksoylu, 2011a, "Water–gas shift activity of ceria supported Au–Re catalysts", *Catalysis Communications*, Vol. 12, pp. 1206-1211.

Çağlayan, B. S., I. I. Soykal and A. E. Aksoylu, 2011b, "Preferential Oxidation of CO over Pt-Sn/AC Catalyst: Adsorption, Performance and DRIFTS Studies", *Applied Catalysis B: Environmental*, Vol. 106, pp. 540-549.

Dias, J. A. C. and J. M. Assaf, 2004, "Autothermal reforming of methane over Ni/γ-Al_2O_3 catalysts: the enhancement effect of small quantities of noble metals", *Journal of Power Sources*, Vol. 130, pp. 106-110.

Ercolino, G., M. A. Ashraf, V. Specchia and S. Specchia, 2015, "Performance evaluation and comparison of fuel processors integrated with PEM fuel cell based on steam or autothermal reforming and on CO preferential oxidation or selective methanation", *Applied Energy*, Vol. 143, pp. 138-153.

Erdinç, E., 2014, *A Study on Kinetics of Methane Oxidative Steam Reforming (OSR) over Pt-Ni/δ-Al_2O_3 Bimetallic Catalysts*, M. Sc. Dissertation, Boğaziçi University.

Erdinç, E., B. S. Çağlayan and A. E. Aksoylu, 2017, "Methane OSR over Pt-Ni/δ-Al_2O_3: Performance and power law type kinetics", *International Journal of Hydrogen Energy*, Vol. 42, pp. 20568-20578.

Eropak, B. M. and A. E. Aksoylu, 2017, "A Reliable Power-Law Type Kinetic Expression for PROX over Pt-Sn/AC under Fully Realistic Conditions", *Catalysis Communications*, Vol. 95, pp. 67-71.

Ferreira, S. L. C., R. E. Bruns, H. S. Ferreira, G. D. Matos, J. M. David, G. C. Brandao, E. G. P. da Silva, L. A. Portugal, P. S. dos Reis, A. S. Souza and W. N. L. dos Santos, 2007, "Box-Behnken design: An alternative for the optimization of analytical methods", *Analytica Chimica Acta*, Vol. 597, pp. 179-186.

Gardemann, U., M. Steffen and A. Heinzel, 2014, "Design and demonstration of an ethanol fuel processor for HT-PEM fuel cell applications", *International Journal of Hydrogen Energy*, Vol. 39, pp. 18135-18145.

Gökaliler, F., B. A. Göçmen and A. E. Aksoylu, 2008, "The Effect of Ni:Pt Ratio on Oxidative Steam Reforming Performance of Pt-Ni/Al_2O_3 Catalyst", *International Journal of Hydrogen Energy*, Vol. 33, pp. 4358-4366.

Gökaliler, F., 2012, *Characterization and Performance Analysis of Fuel Flexible OSR-WGS Catalysts*, Ph. D. Dissertation, Boğaziçi University.

Gökaliler, F., Z. I. Önsan and A. E. Aksoylu, 2012, "Power Law Type Rate Equation for Propane ATR over Pt-Ni/Al_2O_3 Catalyst", *International Journal of Hydrogen Energy*, Vol. 37, pp. 10425-10429.

Heede, R. and N. Oreskes 2016, "Potential emissions of CO_2 and methane from proved reserves of fossil fuels: An alternative analysis", *Global Environmental Change*, Vol. 36, pp. 12-20.

Icardi, U. A., S. Specchia, G. J. R. Fontana, G. Saracco and V. Specchia, 2008, "Compact direct methanol fuel cells for portable application", *Journal of Power Sources*, Vol. 176, pp. 460-467.

Jung, U. H., W. Kim, K. Y. Koo and W. L. Yoon, 2014, "Genuine design of compact natural gas fuel processor for 1-kWe class residential proton exchange membrane fuel cell systems", *Fuel Processing Technology*, Vol. 121, pp. 32-37.

Kalmula, B. and V. R. Kondapuram, 2015, "Fuel processor – fuel cell integration: Systemic issues and challenges", *Renewable and Sustainable Energy Reviews*, Vol. 45, pp. 409-418.

Kolb, G., T. Baier, J. Schurer, D. Tiemann, A. Ziogas, S. Specchia, C. Galletti, G. Germani and Y. Schuurman, 2008, "A micro-structured 5 kW complete fuel processor for iso-octane as hydrogen supply system for mobile auxiliary power units Part II - Development of water gas shift and preferential oxidation catalysts reactors and assembly of the fuel processor", *Chemical Engineering Journal*, Vol. 138, pp. 474-489.

LeValley, T. L., A. R. Richard and M. Fan, 2014, "The progress in water gas shift and steam reforming hydrogen production technologies – A review", *International Journal of Hydrogen Energy*, Vol. 39, pp. 16983-17000.

Malaibari, Z. O., A. Amin, E. Croiset and W. Epling, 2014, "Performance characteristics of MoeNi/Al_2O_3 catalysts in LPG oxidative steam reforming for hydrogen production", *International Journal of Hydrogen Energy*, Vol. 39, pp. 10061-10073.

Mandapaka, R. and G. Madras, 2017, "Zinc and platinum co-doped ceria for WGS and CO oxidation", *Applied Catalysis B: Environmental*, Vol. 211, pp. 137-147.

Moreno, N. G., M. C. Molina, D. Gervasio and J. F. P. Robles, 2015, "Approaches to polymer electrolyte membrane fuel cells (PEMFCs) and their cost", *Renewable and Sustainable Energy Reviews*, Vol. 52, pp. 897-906.

Ni, C., L. Pan, Z. Yuan, L. Cao and S. Wang, 2014, "Study of methane autothermal reforming catalyst", *Journal of Rare Earths*, Vol. 32, pp. 184-188.

Ni, C., Z. Juan, S. Wang, D. Li, C. Zhang, J. Li and S. Wang, 2015, "Study on an integrated natural gas fuel processor for 2-kW solid oxide fuel cell", *International Journal of Hydrogen Energy*, Vol. 40, pp. 15491-15502.

Palma, V., A. Ricca, E. Meloni, M. Martino, M. Miccio and P. Ciambelli, 2016, "Experimental and numerical investigations on structured catalysts for methane steam reforming intensification", *Journal of Cleaner Production*, Vol. 111, pp. 217-230.

Palma, V., A. Ricca, B. Addeo, M. Rae, G. Paolillo and P. Ciambelli, 2017, "Hydrogen production by natural gas in a compact ATR-based kW-scale fuel processor", *International Journal of Hydrogen Energy*, Vol. 42, pp. 1579-1589.

Romero-Sarria, F., S. Garcia-Dali, E. M. Jimenez-Barrera, L. Oliviero, P. Bazin and J. A. Odriozola, 2016, "The role of carbon overlayers on Pt-based catalysts for H2-cleanup by CO-PROX", *Surface Science*, Vol. 648, pp. 84-91.

Ryu, J., K. Lee, H. La, H. Kim, J. Yang and H. Jung, 2007, "Ni catalyst wash-coated on metal monolith with enhanced heat-transfer capability for steam reforming", *Journal of Power Sources*, Vol. 171, pp. 499-505.

Samsun, R. C., J. Pasel, R. Peters and D. Stolten, 2015, "Fuel cell systems with reforming of petroleumbased and synthetic-based diesel and kerosene fuels for APU applications", *International Journal of Hydrogen Energy*, Vol. 40, pp. 6405-6421.

Sato, K., K. Kawano, A. Ito, Y. Takita and K. Nagaoka, 2010, "Hydrogen Production from Bioethanol: Oxidative Steam Reforming of Aqueous Ethanol Triggered by Oxidation of Ni/$Ce_{0.5}Zr_{0.5}O_{2-x}$ at Low Temperature", *Chemistry and Sustainability*, Vol. 3, pp. 1364-1366.

Seo, Y. T., D. J. Seo, J. H. Jeong and W. L. Yoon, 2006a, "Design of an integrated fuel processor for residential PEMFCs applications", *Journal of Power Sources*, Vol. 160, pp. 505-509.

Seo, Y. T., D. J. Seo, J. H. Jeong and W. L. Yoon, 2006b, "Development of compact fuel processor for 2 kW class residential PEMFCs", *Journal of Power Sources*, Vol. 163, pp. 119-124.

Sepehri, S. and M. Rezaei, 2017, "Ce promoting effect on the activity and coke formation of Ni catalysts supported on mesoporous nanocrystalline γ-Al_2O_3 in autothermal reforming of methane", *International Journal of Hydrogen Energy*, Vol. 42, pp. 11130-11138.

Sgrio, M., G. Bollita, G. Saracco and S. Specchia, 2005, "BIOFEAT: Biodiesel fuel processor for a vehicle fuel cell auxiliary power unit - Study of the feed system", *Journal of Power Sources*, Vol. 149, pp. 8-14.

Sharaf, O. Z. and M. F. Orhan, 2014, "An overview of fuel cell technology: Fundamentals and applications", *Renewable and Sustainable Energy Reviews*, Vol. 32, pp. 810-853.

Souza, T. L., C. C. S. Rossi, C. G. Alonso, R. Guirardello, V. F. Cabral and N. R. Camargo, 2014, "Thermodynamic analysis of autothermal reforming of methane via entropy maximization: Hydrogen production", *International Journal of Hydrogen Energy*, Vol. 39, pp. 8257-8270.

Şimşek, E., Ş. Özkara, A. E. Aksoylu and Z. I. Önsan, 2007, "Preferential CO Oxidation over Activated Carbon Supported Catalysts in H_2-rich Gas Streams Containing CO_2 and H_2O", *Applied Catalysis A: General*, Vol. 316, pp. 169-174.

Şimşek, E., M. Karakaya, A. K. Avcı and Z. I. Önsan, 2013, "Oxidative steam reforming of methane to synthesis gas in microchannel reactors", *International Journal of Hydrogen Energy*, Vol. 38, pp. 870-878.

Tiwari, R., B. Sarkar, R. Tiwari, C. Pendem, T. Sasaki, S. Saran, and R. Bal, 2014, "Pt nanoparticles with tuneable size supported on nanocrystalline ceria for the low temperature water-gas-shift (WGS) reaction", *Journal of Molecular Catalysis A: Chemical*, Vol. 395, pp. 117-123.

Trimm, D. L. and Z. İ. Önsan, 2001, "Onboard Fuel Conversion for Hydrogenfuel-Cell-Driven Vehicles", *Catalysis Reviews*, Vol. 43, pp. 31-84.

Vita, A., G. Cristiano, C. Italiano, S. Specchia, F. Cipiti and V. Specchia, 2014, "Methane oxy-steam reforming reaction: Performances of $Ru/\gamma\text{-}Al_2O_3$ catalysts loaded on structured cordierite monoliths", *International Journal of Hydrogen Energy*, Vol. 39, pp. 18592-18603.

Vita, A., G. Cristiano, C. Italiano, L. Pino and S. Specchia, 2015, "Syngas production by methane oxy-steam reforming on Me/CeO_2 (Me = Rh, Pt, Ni) catalyst lined on cordierite monoliths", *Applied Catalysis B: Environmental*, Vol. 162, pp. 551-563.

Wang, J., H. Chen, Y. Tian, M. Yao and Y. Li, 2012, "Thermodynamic analysis of hydrogen production for fuel cells from oxidative steam reforming of methanol", *Fuel*, Vol. 97, pp. 805-811.

Wang, X., N. Wang, J. Zhao and L. Wang, 2010, "Thermodynamic Analysis of Propane Dry and Steam Reforming for Synthesis Gas or Hydrogen Production", *International Journal of Hydrogen Energy*, Vol. 35, pp. 12800-12807.

Wang, X., N. Wang and L. Wang, 2011, "Hydrogen Production by Sorption Enhanced Steam Reforming of Propane: A Thermodynamic Investigation", *International Journal of Hydrogen Energy*, Vol. 36, pp. 466-472.

Welaya, Y. M. A., M. M. El Gohary and N. R. Ammar, 2012, "Steam and partial oxidation reforming options for hydrogen production from fossil fuels for PEM fuel cells", *Alexandira Engineering Journal*, Vol. 51, pp. 69-75.

Yang, M., F. Jiao, S. Li, H. Li and G. Chen, 2015, "A self-sustained, complete and miniaturized methanol fuel processor for proton exchange membrane fuel cell", *Journal of Power Sources*, Vol. 287, pp. 100-107.

Zeng, G., Y. Tian and Y. Li, 2010, "Thermodynamic analysis of hydrogen production for fuel cell via oxidative steam reforming of propane", *International Journal of Hydrogen Energy*, Vol. 35, pp. 6726-6737.